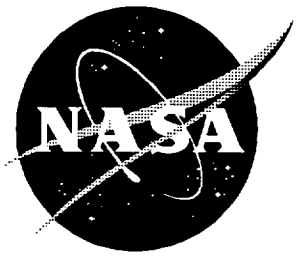

NASA Contractor Report 4742

Producing Foils From Direct Cast Titanium Alloy Strip

T. A. Gaspar, T. A. Stuart, I. M. Sukonnik, S. L. Semiatin, E. Batawi, J. A. Peters, and H. L. Fraser

Contract NAS1-19942
Prepared for Langley Research Center

May 1996

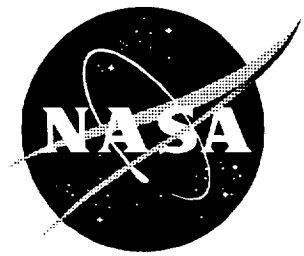

NASA Contractor Report 4742

Producing Foils From Direct Cast Titanium Alloy Strip

T. A. Gaspar and T. A. Stuart
Ribbon Technology Corporation • Columbus, Ohio

I. M. Sukonnik
Texas Instruments, Inc.• Attleboro, Massachusetts

S. L. Semiatin
Wright Laboratories • Wright-Patterson AFB, Ohio

E. Batawi and J. A. Peters
Sulzer-Innotec • Winterthur, Switzerland

H. L. Fraser
Ohio State University • Columbus, Ohio

National Aeronautics and Space Administration
Langley Research Center • Hampton, Virginia 23681-0001

Prepared for Langley Research Center
under Contract NAS1-19942

May 1996

Printed copies available from the following:

NASA Center for AeroSpace Information
800 Elkridge Landing Road
Linthicum Heights, MD 21090-2934
(301) 621-0390

National Technical Information Service (NTIS)
5285 Port Royal Road
Springfield, VA 22161-2171
(703) 487-4650

TABLE OF CONTENTS

EXECUTIVE SUMMARY

This report describes a new paradigm for producing titanium alloy strips: a paradigm not based on conventional ingot metallurgy practices of ingot casting, hot forging, hot rolling, thermal treatments and wet grinding, but based on direct casting a titanium strip in one operation. That single operation is called Melt Overflow Rapid Solidification Technology (MORST) and can potentially replace all of the hot working operations used to produce conventional wrought strip.

The cast titanium strips exhibited different metallurgical microstructures and properties than their wrought counterparts. The as-cast strip may be appropriate for applications which do not require high strength or applications that involve thermal treatments that affect the microstructure. Examples might include turbine engine nozzles or flaps, or low-cost titanium matrix composites (TMC's) processed by vacuum hot pressing or hot isostatic pressing (HIP) for less-demanding non-aerospace applications.

The as-cast titanium strip was ground to foil gauge during the Phase I project. The ground foils retained the cast microstructure and physical properties of the precursor strip. Grinding may be desirable for improving the surface finish of the cast strip or for modifying the strip dimensions. Cast and ground foils may be suited for TMC's if they are consolidated at temperatures and pressures that result in recrystallization of the cast microstructure.

Titanium aluminide foils were successfully produced by hot pack rolling the direct cast Ti-aluminde strip. Hot pack rolling transformed the microstructures of the cast Ti-aluminide strip to microstructures resembling their wrought counterparts. The microhardnesses of the cast and hot pack rolled foils were higher than the as-cast strip, which indicated that the strength of the material increased as a result of pack rolling.

The feasibility of cold rolling the direct cast strip to produce titanium foils was demonstrated on a laboratory scale. Alloys that were successfully cold rolled to foil gauge (125-μm-thick or less) included commercially pure titanium (CP-Ti); Ti-1.25Al-0.8V alloy; Ti-6Al-2Sn-4Zr-2Mo alloy, and Ti-11Al-40Nb (orthorhombic Ti-aluminide). Fully dense foils were produced, with a bright surface finish and low average surface roughness (R_a). In general, the direct cast and cold rolled foils exhibited finer, more uniform microstructures, higher strength, lower ductility, and higher modulus of elasticity than the comparable ingot metallurgy foils.

The potential advantages of producing cold rolled foils from near-net-shape cast titanium strip are lower-cost processing and higher performance foils. Perhaps someday this new paradigm will be adopted by industry and titanium foils will be cold rolled commercially from direct cast titanium strip.

1.0 INTRODUCTION

This project was funded by the National Aeronautics and Space Administration (NASA) Small Business Innovation Research (SBIR) program. The SBIR Phase I project (contract number NAS1-19541) began on 23 January 1992 and was completed on 23 July 1992 with the submittal of the final report entitled " Producing Foils from Direct Cast Titanium Alloy Strip" authored by T.A. Gaspar, J.M. Newman, E. Batawi and J.A. Peters. The Phase II SBIR project (contract number NAS1-19942) technical performance period began on 31 March 1993 and was successfully completed on 31 March 1995 and is the subject of this report.

The production of titanium foils by conventional ingot metallurgy involves casting ingots, hot forging ingots into billets, followed by several hot rolling, heat treatment, and surface grinding sequences to produce plate and strip that is later cold rolled to foil gauge. Among titanium alloys, processing losses can be 50% or more. As a result, titanium foils are expensive to produce commercially and often require long lead times for delivery. The direct cast, rapid solidification approach taken by Ribbon Technology Corporation (Ribtec) has the potential to significantly reduce the cost of titanium foil by eliminating may of the hot working steps required for the ingot metallurgy process. In this approach, titanium strip is cast directly from a melt and then ground or rolled by an appropriate process to foil.

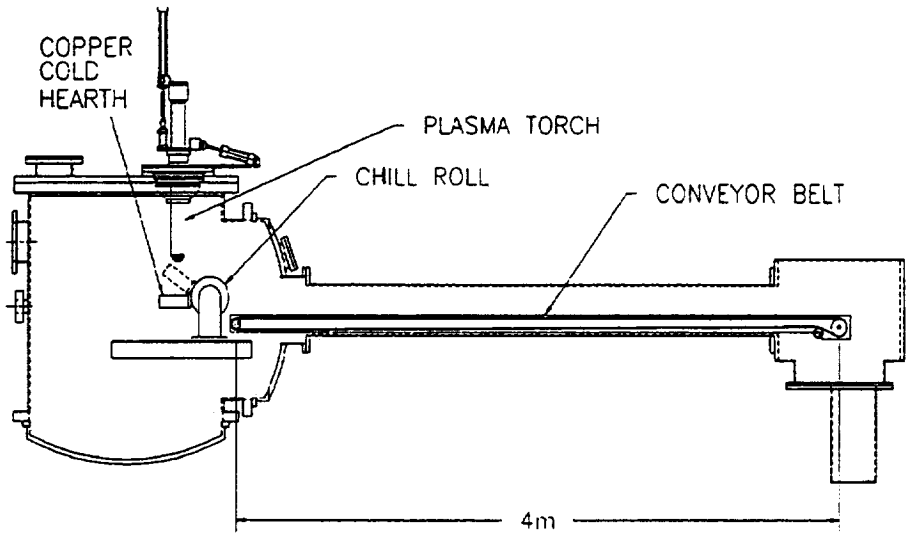

Figure 1.1 - Schematic Diagram of Plasma Melt Overflow System for Casting Titanium Strip

The technique used by Ribtec to cast titanium strip is called the Plasma Melt Overflow Process because it combines transferred plasma arc skull melting in a water-cooled-copper crucible with Melt Overflow Rapid Solidification Technology (MORST). A schematic of the Plasma Melt Overflow system operated at Ribtec is shown in Figure 1.1.

Titanium alloys were placed in the copper cold hearth, with the hearth in a near horizontal position. The process vessel was sealed, evacuated to a pressure of less than 0.01 Torr and filled with argon gas. A helium plasma arc was transferred between the plasma torch and the titanium. The titanium alloys were melted for roughly 15 minutes with the average power ranging from 55 kW to 75 kW. To cast titanium strip, the copper cold hearth was rotated along the circumference of a rotating water-cooled-molybdenum chill roll using the same axis of rotation as the chill roll, to a position of 45 degrees above horizontal with tilting times ranging from 2 s to 5 s. As the hearth rotated about the chill roll, the liquid titanium overflowed a 100-mm-wide by 19-mm-deep slot in the hearth wall adjacent to the chill roll. The liquid solidified upon contact with the rotating chill roll surface to cast strip at rates in the range of 0.75 m/s to 1.5 m/s. The cast titanium strip was collected on a wire mesh conveyor belt moving at the same surface speed as the chill roll. The conveyor was stopped when the strip reached the end and the strip was allowed to cool to room temperature in the inert furnace atmosphere.

During the Phase I SBIR project, Ribtec investigated direct casting of titanium alloy strip including titanium aluminides. The cast strips were ground to foil gage, and retained the cast microstructure and physical properties. Cast and ground strips may be suitable for lower-cost titanium matrix composites (TMC) that are subjected to high-temperature processing which would recrystallize the titanium foils. The feasibility of hot pack rolling direct cast titanium aluminide strip to foil gauge was also investigated during the Phase I SBIR project. The results of the Phase I project are summarized in Section 2.0 of this report.

Hot pack rolling and cold rolling the direct cast titanium alloy strip to foil gauge were investigated during the Phase II SBIR project. Cold rolling the near-net-shape cast strip completely eliminated the need for hot working. Commercially, casting titanium strip to near-net-shape followed by cold rolling to foil gauge may someday expand the number of titanium alloys that can be processed into foils, reduce lead times, lower costs, reduce rolling texture, and result in novel microstructures and properties.

2.0 PHASE I RESULTS AND CONCLUSIONS

The objective of the Phase I SBIR research project was to investigate the feasibility of producing titanium aluminide foils by first direct casting strip using Ribtec's Plasma Melt Overflow Process followed by either wet grinding or hot pack rolling to foil gauge. Titanium aluminide strips of Ti_3Al-based Ti-14Al-21Nb alloy ($\alpha 2$ Ti-aluminide) and TiAl-based Ti-33Al-5Nb-3Cr alloy (γ Ti-aluminide) along with conventional Ti-6Al-4V alloy, were successfully cast into 100-mm-wide by 500-μm-thick strip in batches weighing one kilogram.

2.1 Phase I Results

During Phase I, strips were cast directly onto the chamber floor, resulting in strips that were bent and twisted. Straightening and flattening of the cast titanium strips were required before either grinding or pack rolling. A resistance heating technique was developed to straighten the as-cast titanium alloy strips in the plasma melt overflow furnace using the furnace's DC power supplies. Strips of cast $\alpha 2$ Ti-aluminide were successfully straightened by resistance heating in an inert atmosphere. Samples of cast γ Ti-aluminide strip were successfully creep flattened using conventional procedures. Processing parameters for homogenization, creep flattening and stress relieving the γ-based strips were determined. Heating and cooling rates during this treatment were carefully controlled to avoid micro-cracking in the less ductile γ phase.

The feasibility of grinding Ti-aluminide strip to foil was demonstrated using silicon carbide, aluminum oxide and diamond abrasive belt grinding techniques. The cast and heat treated $\alpha 2$ Ti-aluminide strip was ground into 230-μm-thick strip and the as-cast γ Ti aluminide strip was ground into 100-μm-thick foil. Grinding removed surface irregularities and thereby reduced the variation in thickness and surface roughness of the as-cast strip. Grinding did not increase the carbon or gas content of the strip.

The feasibility of hot pack rolling $\alpha 2$ titanium aluminide strip, cast by Ribtec's plasma melt-overflow process was demonstrated using the Sulzer technology. Foils of a thickness of 70μm were obtained starting with strips 0.5-mm-thick in the as-cast condition and no preliminary heat treatment or surface preparation. The as-received strips were encapsulated in packs containing a calcium-based release agent, shown in Figure 2.1. The packs were heated at a rate of 8°C/min and soaked for 30 min at 1050°C before rolling. The rolling parameters were adapted such that the strain rates were low and gradually increased from 2 s^{-1} to 6 s^{1}. Figure 2.2 shows the typical variation of strain rate and deformation as a function of pack thickness. After each pass, the pack was quickly replaced in the furnace to compensate for heat losses due to contact with the cold rolls. For these initial trials, rolling was performed uniaxially. To achieve the 70-μm-thick foils, typically seven or eight rolling passes were required.

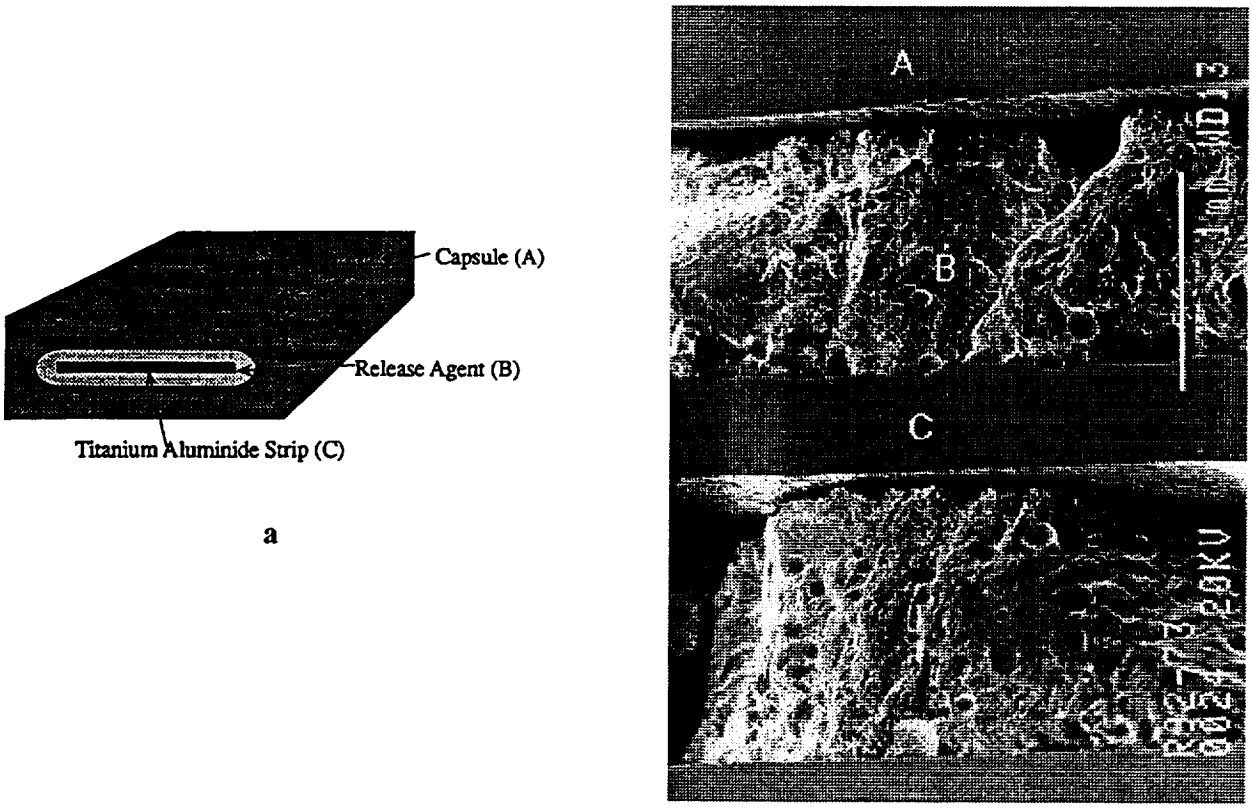

Figure 2.1: (a) Schematic diagram of encapsulated cast Ti-aluminde strip ready for pack rolling. (b) SEM of a sectioned pack showing capsule A, release agent B and cast strip C.

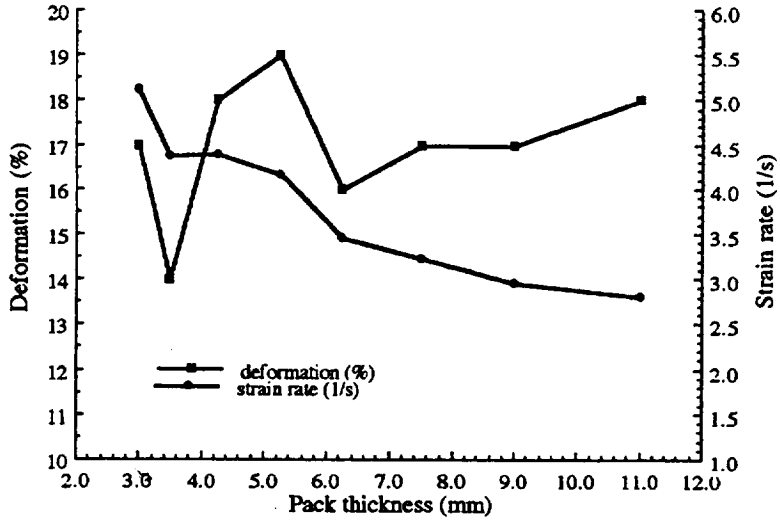

Figure 2.2: Typical variation of strain rate and deformation for the as-cast α2 Ti- aluminide strip as a function of pack thickness during hot rolling.

Pack rolling of the γ-based strip presented more difficulties than the α2-based material. The problems were mainly associated with the use of appropriate capsule materials with characteristics such as strength and deformation at temperatures close to or above 1200°C, similar to those of γ Ti-aluminide. The capsule was fabricated from a cobalt-base material that was successfully used to pack roll an investment cast, 3-mm-thick, Ti-33Al-5Nb-3Mn alloy preform down to 1-mm-thick strip at Sulzer-Innotec.

The initial trials were performed on the as-received cast γ-based titanium aluminide strips. Samples 2.2 cm square were cut from relatively flat areas of the strip and encapsulated with the appropriate amount of release agent. No homogenizing heat treatment or surface preparation was performed on the cast strips for these initial trials. The packs were heated to the rolling temperature at a rate of 5°C/min and soaked for 30 min before rolling. The rolling parameters were designed to maintain a low strain rate which was increased gradually from approximately 2 s^{-1} to 6 s^{-1} near the end of the rolling sequence. Rolling attempts were carried out at 1200°C, 1250°C and 1300°C. At all three rolling temperatures, the cast γ-based strip failed into small pieces approximately 3.3 mm in size.

The failure of the γ Ti-aluminide foil was initially attributed to the rough surface of the as-cast strip. It was thought that the depressions in the foil surfaces reflected by elevated R_m (maximum peak-to-trough height) values (Table 2.1) acted as notches and contributed to failure of the strip during rolling. A second series of pack rolling trials were performed at 1200°C and 1250°C, on homogenized, creep flattened and surface ground cast γ Ti-aluminide strips. The intention was to eliminate the failure of the cast titanium aluminide strip due to its rough surface topography and microstructural characteristics. The strain rates were similar to those of the initial trials. However, the attempts to hot pack roll the cast and ground γ Ti-aluminide strips were also unsuccessful.

The direct cast strips and foils were characterized in terms of surface roughness measurements, microstructural analyses and chemical composition in the as-received, heat treated and pack rolled (thermo-mechanically processed) conditions.

Topographic morphology. The Ti-aluminide strips were cast on a knurled chill roll. For both α2 and γ Ti-aluminide strips, the chill cast surface of the strip replicated the diamond knurl pattern on the chill roll surface. The chill-cast side of the strip was rougher than the free-side. The α2 strip was characterized by a far smoother free cast surface than that of the γ-based strip which contained numerous dimples. The diamond pattern observed on the free cast surface of the strips was associated with the chill cast side of the strip. The average roughness height, R_a, and ten point roughness height, R_z, for three 15-mm-long scans as well as the maximum peak-to-trough heights, R_m, detected over the three scans are listed in Table 2.1. As suggested by the values of R_a, the frequency of the peak to trough heights were elevated. For the as-cast γ-based strip, approximately 600-μm-thick, variations in thickness of more than 30μm on either side of the strip were measured.

Table 2.1 Surface Roughness Measurements of Cast Ti-Aluminide Strips

Alloy	Surface	Direction	R_z (μm)	R_a (μm)	R_m (μm)
α2	Chill Side	Longitudinal	30.9	5.07	54.1
		Transverse	30.4	5.23	55.8
α2	Free Side	Longitudinal	16.2	2.43	19.3
		Transverse	15.9	2.33	21.7
γ	Chill Side	Longitudinal	31.6	5.47	40.0
		Transverse	36.6	6.97	47.2
γ	Free Side	Longitudinal	26.7	5.30	31.6
		Transverse	25.8	4.93	47.3

Key: α2 = Ti-14Al-2lNb alloy; γ = Ti-33Al-5Nb-3Cr alloy

Gas, carbon and sulphur analysis. The carbon, hydrogen, nitrogen, oxygen and sulphur content of the strips and foils was measured at several stages of processing of the titanium aluminide to determine if interstitial contamination of the intermetallic-based materials occurred. These measurements for the cast Ti-aluminide strips at different stages of processing are summarized in Table 2.2.

The carbon and gas content of the α2 starting materials, cast strip, and cast + ground strip indicated that no contamination occurred during these unit operations. Grinding was performed with silicon carbide at MetalCenter and there was no evidence of increased carbon content in the ground foils. There was a slight increase in oxygen and carbon after pack rolling, presumably from contact with the release agent.

The carbon and gas content of the γ Ti-aluminide showed a modest (100 ppm - 200 ppm) increase in carbon and oxygen after casting. Again, the strip ground with silicon carbide abrasives at MetalCenter showed no signs of increased carbon or gases. More tests are needed to evaluate gas content of the γ Ti-aluminide foils ground with diamond superabrasives at Ribtec.

Microhardness. Microhardness measurements of as-cast and thermo-mechanically processed strips were performed to provide a preliminary assessment of the influence of pack rolling on the mechanical properties of the strips. Table 2.3 summarizes these values for the α2 and the γ alloys. Both strips exhibited an increase in strength due either to microstructural modifications and refinement through dynamic recrystallization or deformation, or retained work-hardening as a result of the rapid cooling after the last rolling pass in the mill.

Table 2.2 Carbon, Oxygen, Hydrogen, Nitrogen, and Sulphur Content of Cast Strips and Foils

Alloy	Condition	C (wppm)	O (wppm)	H (wppm)	N (wppm)	S (wppm)
α2	ingot	200	700	28	117	n/a
	cast strip	130	775	30	122	n/a
	cast strip*	257	705	43	154	n/a
	ground M	160	706	n/a	99	n/a
	packrolled	674	909	80	n/a	11
γ	ingot*	85	494	30	50	4
	cast strip	320	580	19	61	n/a
	cast strip*	193	763	36	35	7
	ground M	230	576	n/a	57	n/a
	ground R	n/a	753	n/a	108	n/a

Key: α2 = Ti-14Al-2lNb alloy; γ = Ti-33Al-5Nb-3Cr alloy; M = MetalCenter; R = Ribbon Technology; *Analysis preformed at Sulzer-Innotec, Winterthur, Switzerland; all other measurements performed by The Duriron Company, Dayton, Ohio (average of three measurements).

Table 2.3: Microhardness of Cast Strip and Pack Rolled Foils

Alloy	Condition	Vickers Hardness (300 g)
α2	as-cast strip	416±15
	packrolled, 85% reduction	471± 9
γ	as-cast strip	355± 9
	packrolled; 75% reduction	400±15

Key: α2 = Ti-14Al-2lNb alloy; γ = Ti-33Al-5Nb-3Cr alloy.

Metallography of α2 Ti-aluminides. Figure 2.3 shows back scattered electron micrographs of the transverse microstructure of the cast α2 Ti-aluminide strip. The as-cast α2 strip consisted of a Widmanstätten-type microstructure, with colony size ranging from 5μm to 15μm. No distinct variation in the microstructure was observed from the chill-cast surface (bottom in Figure 2.3 a) to the free-cast surface of the strip, suggesting that the solidification rate was relatively uniform during plasma melt overflow casting. Figure 2.3 b shows small pores, approximately 2μm to 8μm in diameter, found scattered randomly throughout the

structure.

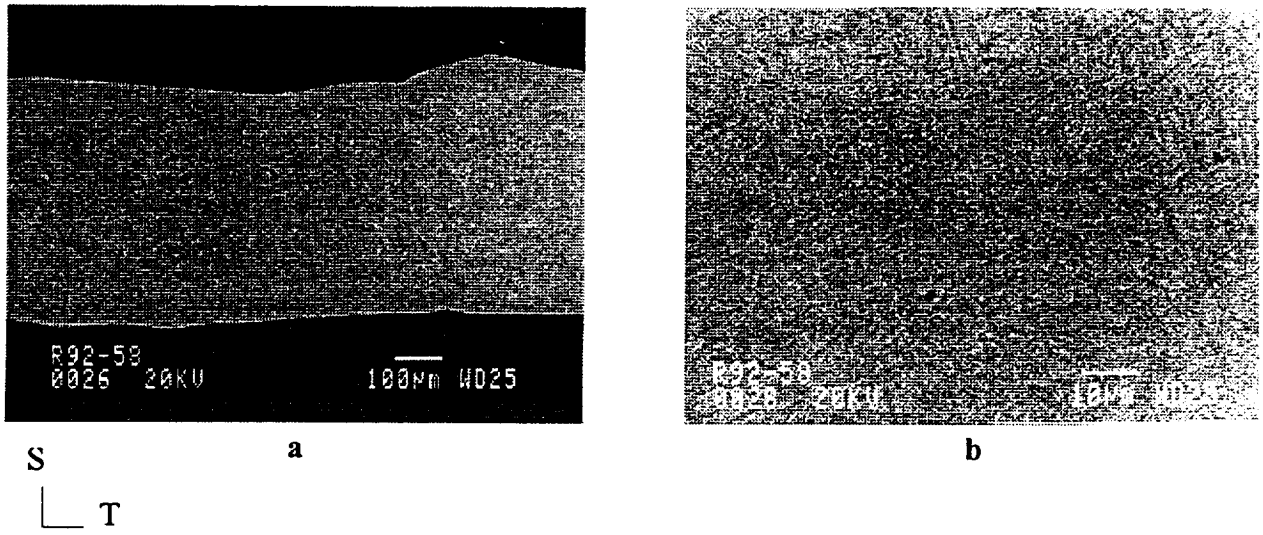

Figure 2.3. Scanning electron micrographs of transverse section of as-cast α2 Ti-aluminide strip; (a) low magnification (b) high magnificiation.

Figure 2.4 a shows the as-cast α2 Ti-aluminide strip before and after pack rolling. The dark grey areas of the pack rolled foil (bottom) are due to the presence of the release agent. In the near-center of the pack, where the release agent debonded from the titanium aluminide, the metallic surface of the foil may be seen.

Figure 2.4 b shows a scanning electron micrograph of the rolled foil still in it's pack: the dark grey region (A) represents the release agent; the light grey region is the foil. The initial as-cast surface roughness and internal porosity of the as-cast strip were not found to be deleterious to the quality of the pack rolled foil. However, as can be seen in Figure 2.5, the surfaces of the pack rolled foil were rough after rolling. The scale of these irregularities was of no severe consequence, since it was standard practice to lightly surface grind the foils after pack rolling to remove any remaining release agent from the foil surfaces. Thermomechanical treatment resulted in the elimination of the internal porosity, as well as a reduction in the scale of roughness of the as-cast strip. The microstructure consisted of a high volume fraction (40-50%) of globular and equiaxed α2 grains, 5μm to 10μm in size, dispersed within a B2 matrix. The microhardness increased from approximately 415 Hv for the as-cast strip with a Widmanstätten microstructure to 470 Hv for the fine, equiaxed α2/B2 microstructure after pack rolling.

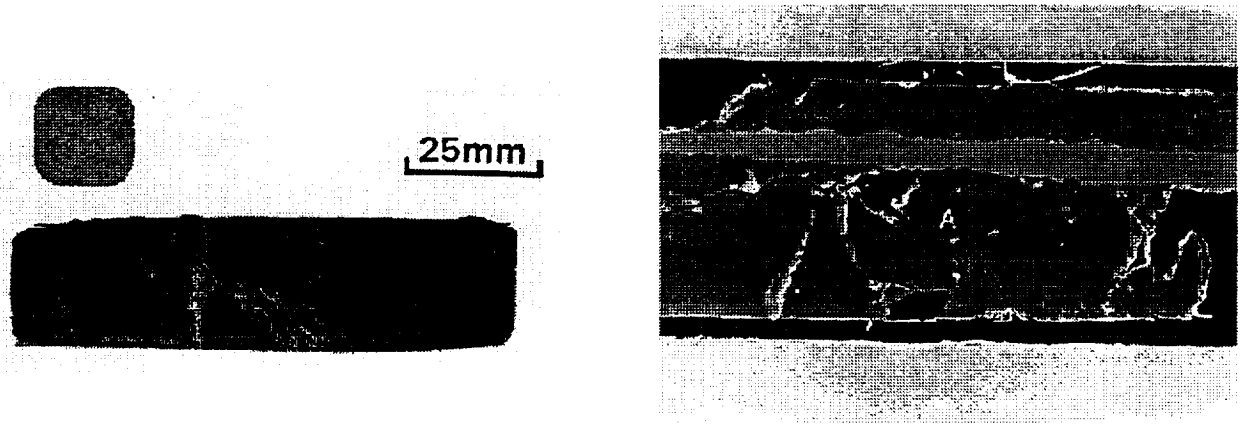

Figure 2.4. (a) Optical macrograph of α2 Ti-aluminide strip before and after pack rolling. A small 2 cm x 2 cm sample in the as-cast condition, above, and pack rolled at 1050°C to a final thickness of 70μm. (b) Scanning electron micrograph of transverse section of the pack rolled foil still in it's pack. The darker grey region A represents the release agent.

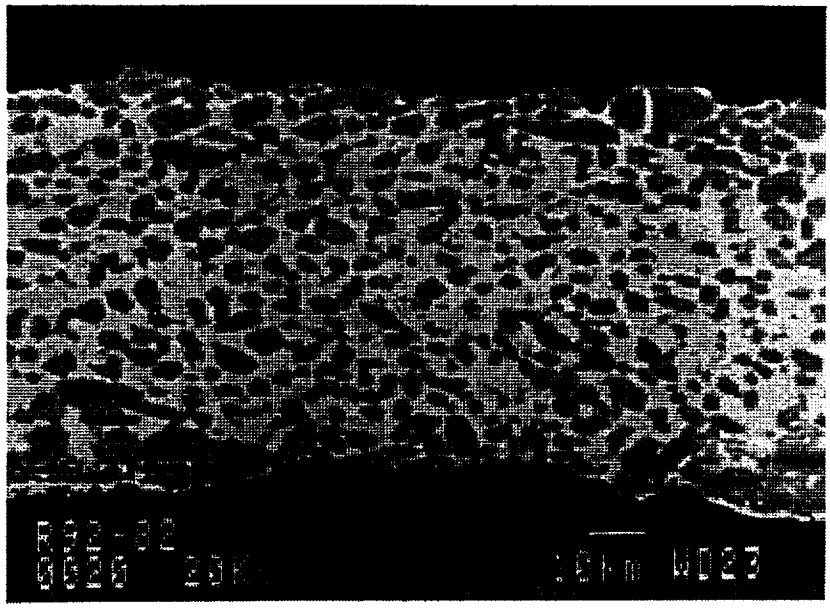

Figure 2.5. Scanning electron micrographs (BSE) of the transverse microstructure of the α2 ti-aluminide foil after pack rolling. The structure consisted of equal volume fractions of globular α2 (dark phase) in a B2 matrix.

Metallography of γ Ti-aluminides. Figure 2.6 shows a transverse section of the as-cast γ-based titanium aluminide strip. The chill-cast surface of the 500-μm-thick to 600-μm-thick strip contained a high volume fraction of large pores approximately 20μm to 50μm in size. The presence of these pores may have been due to a high coefficient of thermal expansion for the γ-based alloy which resulted in shrinkage pores during solidification. The columnar orientation of the grains in some areas of the longitudinal section of the strip suggested that some directional solidification occurred. The microstructure of the as-cast strip consisted of a very fine lamellar structure, hardly resolved by scanning electron microscopy. The lamellar spacing was estimated at 0.5μm to lμm. The lamellar grains had fuzzy boundaries, typical of cast Ti-33Al-5Nb-3Cr alloy. Between these grains a segregated phase (dark appearance in back scattered electron contrast) was detected, Figure 2.7. Comparison of the EDS spectra of the general composition of the alloy taken at low magnification with EDS spectra from localized spot analysis of the dark phase suggested that the dark regions were richer in aluminum than the matrix. This suggested that during solidification "peritectic tumbling", leading to interdendritic segregation of an aluminum-rich phase might have occurred. However, the scale of the segregation observed was not large. The segregation was found to be localized to some areas of the strip with other areas being totally free from segregation. This suggested that either the cooling rate during solidification was non-uniform or that solid state cooling of the strip on the floor of the process vessel was non-uniform. As the strip piled up in the bottom of the vessel, layers of the as-cast strip in contact with itself may have cooled slower than strip that was touching the water-cooled walls of the vessel or strip that was not contacting any solid surface.

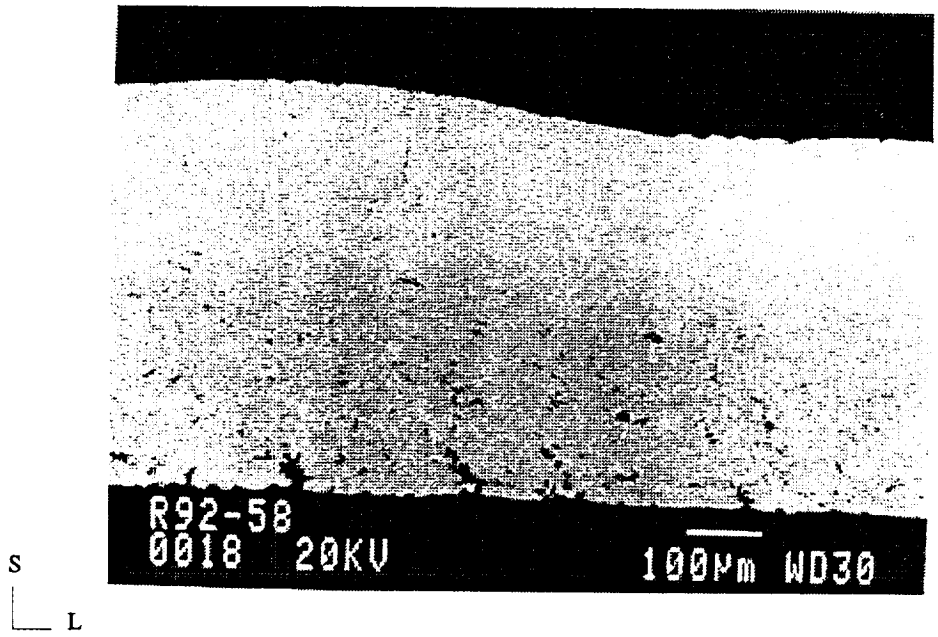

Figure 2.6. Scanning electron micrograph (BSE) of the longitudinal microstructure of the as-cast γ Ti-aluminide strip.

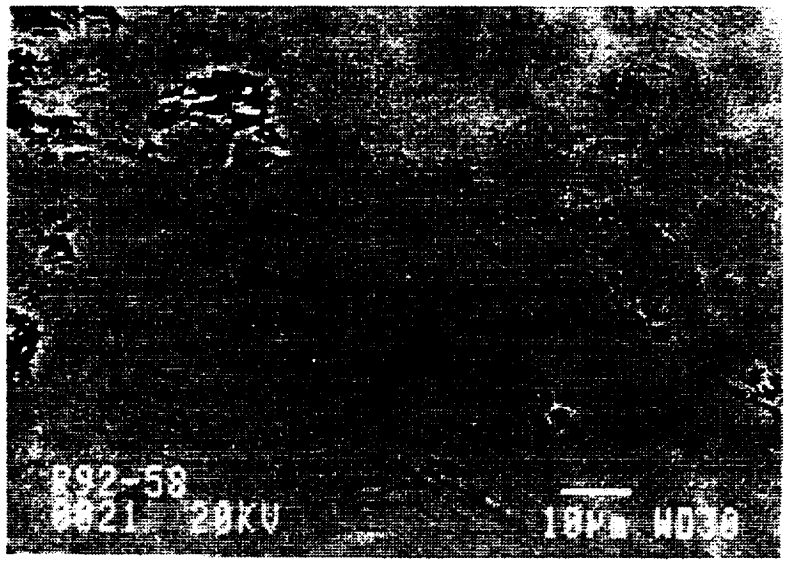

Figure 2.7. SEM micrograph of the center portion of the cast γ strip showing a fine lamellar structure with fuzzy boundaries.

Figure 2.8a shows the microstructure of a longitudinal section of the cast γ Ti-aluminide strip after pack rolling at 1200°C with a total reduction in thickness of 75%. The microstructure evolved from the as-cast lamellar structure shown in Figure 2.7 to an extremely fine, degenerated duplex structure of γ and transformed α2 grains shown in Figure 2.8b. The γ grains were approximately 5μm to 15μm in size. The α2 phase was in the form of either degenerated grains, 2μm to 5μm in size or roughly parallel lamellae approximately

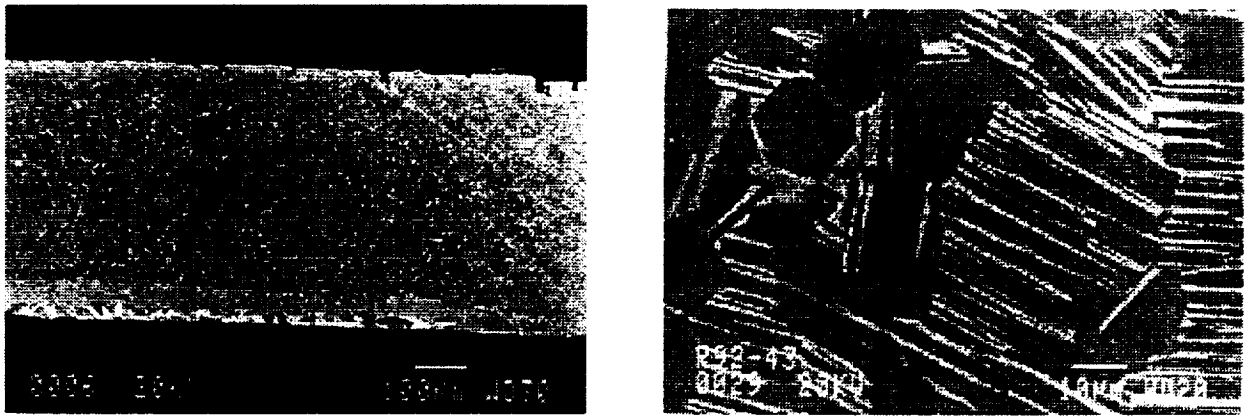

Figure 2.8. Scanning electron micrographs (BSE) of a cast and pack rolled γ Ti-aluminide strip reduced 75% in thickness at 1200°C.

1-μm-thick. This refined microstructure was extremely encouraging. Furthermore, no evidence for micro cracking in the γ phase was observed. However, the foil surfaces revealed a lighter phase in back scattered electron contrast indicative of the presence of some α2 case formation.

2.2 Phase I Conclusions

Based on the results of the Phase I investigation of the feasibility of producing foils from direct cast titanium aluminide strip, the following conclusions were made:

The Plasma Melt Overflow process was capable of casting 500- μm -thick strip from both α2 and γ Ti-aluminides. The titanium strips were cast onto the floor of the process vessel and were twisted and buckled. The as-cast strips exhibited high surface roughness and variations in thickness across the width of the strip and along it's length. The carbon and gas content of the cast strip was low. The as-cast Ti-aluminde strips exhibited relatively fine microstructures with some internal porosity. Segregation of aluminum-rich phases, probably due to peritectic tumbling during solidification was observed in some areas of the as-cast γ Ti-aluminide strips but not in other sections. Microsegregation may have resulted from non-uniform cooling in the solid state.

The cast α2 Ti-aluminide was successfully flattened and straightened by resistance heating the strip in an inert environment in the plasma melt overflow furnace. Processing parameters for homogenization, creep flattening and stress relieving the γ-based strips were determined. Heating and cooling rates during creep flattening γ Ti-aluminide were carefully controlled to avoid micro-cracking of the less ductile γ phase.

The Phase I results indicated that, by using wet grinding or hot pack rolling technology, it was technically feasible to further process the direct cast Ti-aluminide strips to foil gage. The feasibility of wet grinding the as-cast and cast + heat treated α2 and γ Ti-aluminide strips to foils approximately 100-μm-thick was demonstrated. Grinding reduced the variation in thickness and reduced the surface roughness of the as-cast strip. Grinding did not appear to contaminate the strip with carbon or gasses.

Pack rolling technology was used to fabricate α2 Ti-aluminide foils from direct cast strip. Foils 70-μm-thick, having a uniform α2/B2 microstructure with little oxygen pick-up were produced. Pack rolling of the γ-based materials was less successful, however. A combination of factors such as segregation in the as-cast state, residual internal stresses, rough surfaces, elevated strain rates during rolling, and incompatibility in high temperature deformation characteristics between the pack material and the γ-based strip may have led to failure of the γ Ti-aluminide foils during hot pack rolling.

3.0 PHASE II TECHNICAL OBJECTIVES AND APPROACH

The objective of the Phase II research project was to produce high quality, cost effective titanium alloy foils from strip cast by Melt Overflow Rapid Solidification Technology (MORST). The focus was on high temperature titanium alloys that are commercially unavailable in foil form using conventional ingot metallurgy techniques. Ribtec's approach was to cast a relatively low cost, near-net-shape strip using the plasma melt overflow process then roll the cast strip into foils. Obviously, turnaround times and costs increase with increasing numbers of unit operations required to obtain foils, therefore, it was desirable to keep the foil processing as simple and as cost-effective as possible. The Phase I research project demonstrated that it was feasible to produce titanium alloy foils by wet grinding or pack rolling strip cast by the melt overflow process; Phase II addressed whether titanium alloy foils could be produced by cold rolling the cast strip.

Ribtec's approach to improving the quality of the as-cast strip cast by MORST was to investigate casting surfaces, optimize the melting and casting parameters for each alloy and to collect the cast strip on a mesh belt conveyor. The thickness uniformity of the cast strip depended on the hearth tilting rate and the casting speed. These parameters were optimized for each alloy investigated to cast strip with greater thickness uniformity. Greater flatness of the cast strip was achieved by collecting the strip on a conveyor belt instead of letting the strip fall to the bottom of the process vessel and buckle. The collection system also improved the uniformity of cooling of the strip after casting.

The Phase I research project produced foils from the direct cast strip by surface grinding and by hot pack rolling. Foils produced by grinding the cast strip retained the cast microstucture and physical properties. Hot pack rolling direct cast strip resulted in foils with more conventional wrought microstructures, however, the pack rolling process was considered to be relatively expensive because it involved creep flattening, encapsulation, thermal treatments, hot rolling, and surface grinding to produce foils. Cold rolling direct cast strip was considered the most economical way to produce foils and was therefore the focus of the Phase II research project.

Work Breakdown Structure. The Phase II research project was divided in five separate tasks as follows:

Task I: Modify plasma melt overflow system.
Task II: Process experiments.
Task III: Direct rolling.
Task IV: Pack rolling.
Task V: Evaluation.

Tasks I and II were performed in the NASA-owned plasma melt overflow furnace at Ribbon Technology Corporation (Ribtec), Columbus, Ohio. Task III was performed at Texas

Instruments, Materials and Controls, Attleboro, Massachusetts. Task IV was performed at Wright Laboratory, Wright-Patterson AFB, Ohio. Task V was performed by Texas Instruments, Wright Laboratory, and Professor Hamish Fraser at the Ohio State University, Columbus, Ohio. The technical performance period began on April 1, 1993 and ended on March 30, 1995.

4.0 SYSTEM MODIFICATIONS

Numerous modifications were made to NASA's plasma melt overflow furnace during the Phase II project. Relocating the apparatus to a new factory addition gave the opportunity to overhaul all of the operating systems. Improvements to the control circuitry, water system, and hydraulic system enhanced operation and performance of the overall system. In addition, major mechanical changes were designed and installed to improve casting and facilitate collection of continuous cast strip.

Chill Roll Caster - A new water-cooled molybdenum chill roll assembly was built to improve casting performance by reducing mechanical vibrations and forcing centrifugal cooling for maximum thermal transfer, Figure 4.1. The power transmission design allowed the chill roll to be machined on its own bearings to eliminate eccentricity and therefore mechanical vibrations from the angular momentum. Replacing the chain driven system with poly-v belts and sheaves also reduced this phenomena. The 160-mm-wide, 241-mm-diameter chill roll could be readily machined to change the surface preparation for experimentation.

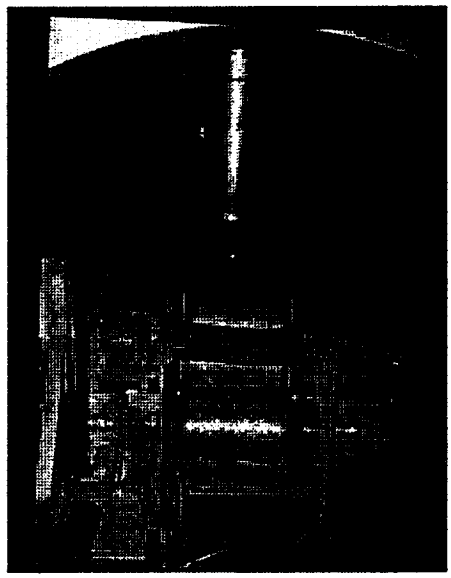

Figure 4.1. Chill Roll Caster Assembly as seen from open front door of process vessel.

The chill roll caster was turned 180° so that it would cast the strip towards the door of the process vessel, and centered symmetrically about the casting axis to align all the system components. The top plate of the process vessel was also removed and rotated slightly to match the plasma torch axes with the casting axis. The operator could stand at the rear of the vessel and directly see the operation of the plasma torch.

Collection System - The front door to the process vessel was removed and a 406 mm diameter access port was fabricated in its center. A collection system was fabricated consisting of a poly-V belt driven, stainless steel wire mesh conveyor belt, 4m long by 200mm

wide, mounted within a 300-mm-square, carbon steel tube sealed at one end. The conveyor belt and the tube are mounted on a moveable frame. The open end of the tube is bolted to the access port once the door to the main vessel is secured. The conveyor is driven from outside the tubing via a rotary feedthrough and matches surface speed with the chill roll by a digital programmable control system following the caster's drive motor, Figure 4.2.

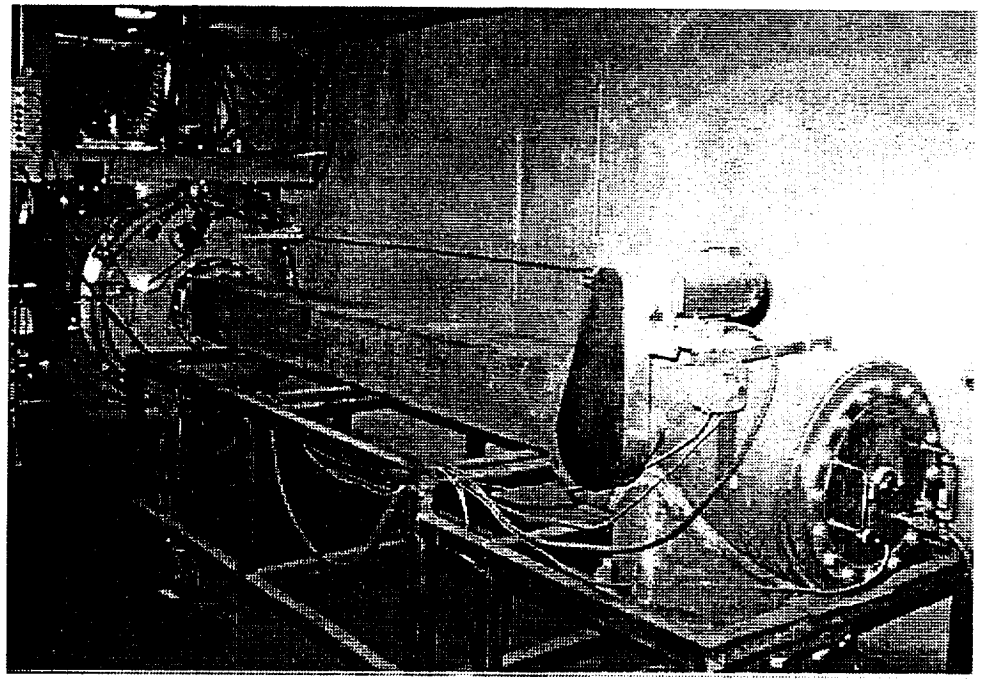

Figure 4.2. Collection System bolted to access port of process vessel.

Casting System - The fixture for mounting the water-cooled copper hearth was improved to ease setting the gap between the hearth lip and the rotating chill roll. The tilting tray system for pouring the melt pool over the chill roll was refabricated and designed to rotate about the chill roll's centerline by using the bearings of the caster's water unions.

To resurface the chill roll, the entire caster was removed from the process vessel, transported to a machine shop, and fixtured so that the chill roll surface could be turned while still mounted in its bearings to ensure concentricity. Every machining finish was tested with a profilometer to standardize a surface prep starting point. A surface treatment was then applied to the chill roll. Knurl patterns, sandblasted finishes, chemical etching, and rotary surface peening (RotoPeen) were all experimented with. Most of the titanium alloy strips were cast on either a knurled and a Roto-Peened chill roll.

5.0 MATERIALS

Six different alloys were cast into strip during the Phase II research project. The six alloys were:

- CP-titanium
- Ti-1.25Al-0.8V alloy
- Timetal™ -1100 alloy
- Ti-6Al-2Sn-4Zr-2Mo alloy
- Ti-11Al-40Nb (Ti-22Al-23Nb at%) alloy
- Ti-31Al-5Nb-3Cr (Ti-45Al-2Nb-2Cr at%) alloy

The initial plasma melt overflow process experiments were to be performed with CP titanium. However, it was estimated that approximately 20% Ti-6Al-4V alloy scrap was mixed with CP titanium scrap to form the resulting Ti-1.25Al-0.8V alloy. The alloying was unintentional and was not discovered until the alloy strip had been cast, cold rolled and evaluated. After the alloy was discovered, another lot of CP titanium scrap was ordered and cast into strip.

Timetal™ -1100 is a near-alpha alloy designed to be used at temperatures up to 600°C. The composition range of Timetal™ -1100 is: (wt %) 5.5% to 6.6% Al; 2.4% to 3.0% Sn; 3.5% to 4.5% Zr; 0.35% to 0.5% Si; 0.35% to 0.5% Mo and 900 wppm maximum oxygen. Cracking was a problem with the Timetal™ -1100 cast strip, so experiments were performed to cast Ti-6Al-2Sn-4Zr-2Mo alloy strip, which has a similar composition, to compare the two alloys.

The Ti-11Al-40Nb alloy is based on the ordered orthorhombic titanium aluminide phase Ti_2AlNb. The orthorhombic Ti-aluminides are currently receiving significant attention for titanium matrix composites (O TMC's). The low yields of wrought orthorhombic foils make alternative processes attractive. Wrought foils exhibit texture because of large amounts of unidirectional rolling. By starting with a cast strip, the amount of cold rolling to produce strips is reduced, which may result in less texture.

The Ti-31Al-5Nb-3Cr alloy is based on the ordered TiAl phase (γ Ti-aluminide). γ Ti-aluminides offer significant weight savings in aircraft engines by potentially replacing nickel-based superalloys. In addition to low density, the γ Ti-aluminides exhibit high temperature strength and oxidation resistance, but have poor room temperature ductility.

6.0 EXPERIMENTAL PROCEDURES

6.1 Casting Procedures

After the modifications had been made to the system, the operating procedure for the plasma melt overflow furnace was as follows:

1) The furnace was cleaned, and the filters for the pressure relief valve and the vacuum foreline were replaced. The water-cooled copper hearth was adjusted to leave a gap between the hearth and chill roll; the gap width depending on the alloy to be cast. Approximately 6 kgs of titanium was placed inside the hearth for melting. Fresh stainless steel wool was applied to the chill roll wiper, and heated with hot air to burn off any oil residue. A molybdenum foil scraping blade was clamped to the caster assembly as a bridge between the chill roll and the steel mesh conveyor belt. The hydraulics to raise the tilting tray were adjusted to displace the tray through its arc in a set time clocked with a stopwatch; the tilt time depending on the alloy to be cast. The torch was positioned within 1 cm of the titanium charge.

2) The door to the furnace was closed and bolted down. The collection system was rolled into place and bolted to the access port on the door. The vacuum pump was turned on and the foreline valve was opened.

3) When the pressure was in the range of 0.01 to 0.02 torr, the foreline valve was closed and the vessel was filled with argon to a pressure of approximately 1 bar. The vacuum pump was turned off.

4) The water and hydraulic systems were turned on. The helium plasma gas was turned on and the pressure adjusted to 2 bars. The power supplies were turned on.

5) The high voltage arc starter was activated simultaneously with the stopwatch on the video recorder. As soon as an arc was established, the torch was raised to a standoff of 75 mm. The arc current was maintained between 400 amperes and 500 amperes. The chill roll was rotated slowly and the conveyor was activated to follow the surface speed of the chill roll.

6) A 12 to 15 minute melt-in pattern was established as follows: for approximately 2 min loose scrap was melted into the original skull pool, for the next 4 min the torch was oscillated side to side at the rear of the hearth, then for the last 6 min a box path was followed going from the center to one side of the hearth, from the back up to the front of the hearth, across the front to the other side, then from the front to the back. Figure 6.1a shows a photograph taken during plasma arc melting of a Ti-6Al-2Sn-4Zr-2Mo alloy.

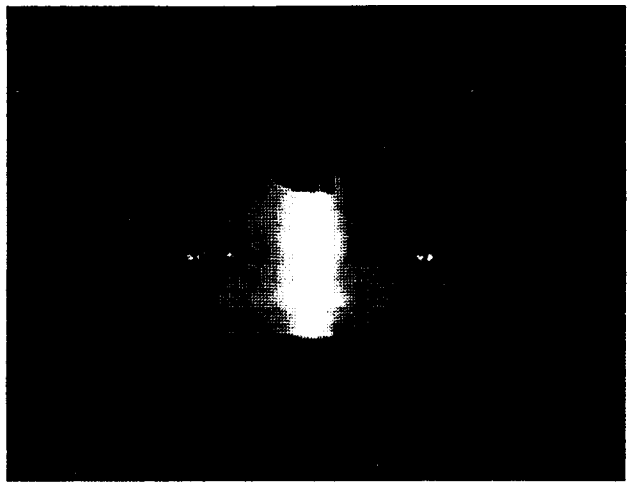

(a)

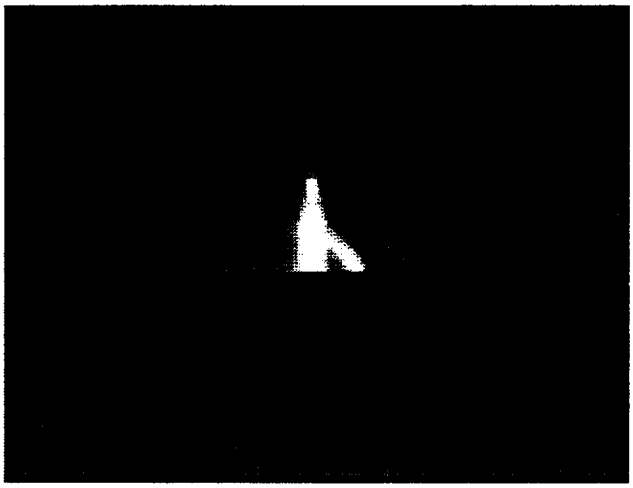

(b)

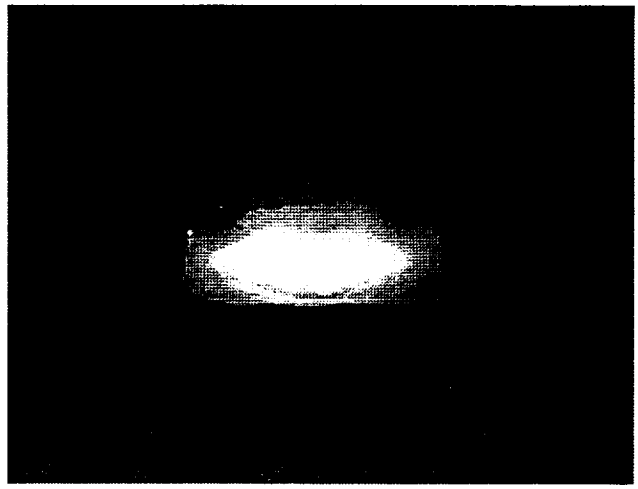

(c)

Figure 6.1: Photographs of (a) plasma arc melting; (b) tilting the hearth and (c) skull after torch shut-off.

7) The chill roll casting speed was set to the desired surface speed. The operator's assistant took position at the rear of the collection system to stop the conveyor when the cast strip reached the end of the belt. The torch was brought back to the center of the hearth and the hearth was tilted to cast titanium strip as the plasma torch was raised to avoid contact with the skull, Figure 6.1b. The torch was shut off after tilting (Figure 6.1c). The conveyor was stopped when it was visually observed through the quartz viewport at the rear of the collection vessel that the strip had reached the end of the conveyor.

8) The chill roll was rotated slowly until the hearth water temperature fell below 27° C. The vacuum foreline valve was opened and the vacuum pump was turned on. The vacuum

pump was turned off after reaching a pressure of 350 torr. The chamber was filled with air by opening the ball valve at the top of the chamber. The collection system was unbolted from the door, and the strip was removed from the belt, Figures 6.2a and 6.2b.

(a) (b)

Figure 6.2: Cast strip (a) lying in collection system and (b) removed from collection system.

6.2 Pack-rolling Procedures.

To determine the alpha transus and a possible window for the flat rolling trials, samples of as-cast γ Ti-aluminide strip G12 were cut, wrapped in tantalum foil, encapsulated in quartz tubes with titanium chips (evacuated and filled with argon), and heat treated at temperatures of 1232°C; 1277°C and 1343°C for one hour followed by air cooling. These temperatures were chosen to span a range both above and below the nominal alpha transus temperature for the Ti-30.8Al-4.7Nb-2.6Cr alloy (viz., T_α=1300°C).

Subsequently, six 89-mm-square preforms of Ti-30.8Al-4.7Nb-2.6Cr alloy were EDM-ed from direct cast strip G12 and creep flattened at a temperature 1232°C for 3 hours under vacuum. After creep flattening, one G12 preform was analyzed for carbon and gases. Four preforms labeled G12-1 through G12-4 were delivered to Wright Laboratory for pack-rolling.

The direct cast γ titanium aluminide preform thicknesses, cover dimensions, initial and final pack thicknesses, and rolling parameters are summarized in Table 6.1. Based on the metallographic results of the thermal treatments of the cast γ Ti-aluminide strip and prior hot pack rolling experience with ingot metallurgy γ alloy ingot and plate, two hot pack-rolling trials for the direct cast Ti-30.8Al-4.7Nb-2.6Cr alloy thin strip were conducted using a preheat furnace temperatures of 1230°C and 1250°C. The packs were heated in a furnace to 926°C, held for 20 minutes, then brought up to the preheat temperature and held for 30 minutes. The pack was removed from the furnace, rolled at 125 mm/s in a two-high mill, and

returned to the furnace for 2 to 3 minutes before the next rolling pass (Figure 6.3).

a b

Figure 6.3: Hot pack (a) entering and (b) exiting rolling mill.

The thickness of the direct cast γ preforms was not uniform. In addition, the two direct cast preforms had a non-negligible amount of porosity, some of which was surface connected. To assess the effect of material condition on rollability, wrought Ti-31.2Al-4.7Nb-2.6Cr alloy preforms were also fabricated from cast + HIP'ed + homogenized ingot material which was isothermally pancake forged to a 6:1 reduction at 1150°C and then recrystallization heat-treated at 1200°C for 8 hours to yield a fine, equiaxed γ grain microstructure. Two slices, each approximately 0.5-mm-thick, were EDM'ed from the pancake, hand lapped, and canned as before. The cans comprised Ti-6Al-4V alloy picture frames and covers and 0.75-mm-thick tantalum interlayers; a CaO parting was used between the interlayers and the titanium aluminide workpiece. The can covers were either 3.75 mm thick (preform IM-1) or 1.5 mm thick (preform IM-2). The two different cover thicknesses were selected to assess the effect of secondary (rolling direction) stresses generated via pack rolling on workability. For preforms IM-1 and IM-2 , the rolling/reheat temperature was 1250°C; reduction per pass was 10 to 12 percent; and the rolling speed was 125 mm/s. After a total reduction of either 3.5:1 (preform IM-1) or 2:1 (preform IM-2), rolling was stopped, and the packs were slow cooled in vermiculite and then cut open to examine the condition of the workpiece.

Two final preforms (labeled IM-3 and IM-4) were EDM-ed from the same forged-and-recrystallization heat treated Ti-31.2Al-4.7Nb-2.6Cr alloy material used in the previous two experiments. These preforms were EDM-ed to approximately 0.75-mm-thick, thus allowing sufficient stock to ensure complete removal of the recast layers during grinding to a 0.5 mm final preform thickness. Preforms IM-3 and IM-4 were canned and rolled as before, except that CaO was used as a parting agent for IM-3, and CaF_2 was used for the other.

Table 6.1: Pack-Rolling Parameters on γ Ti-aluminide Preforms*

Sample ID	Preform Thickness	Cover Thickness	Initial Pack Thickness	Final Pack Thickness	Rolling Temp.	Rolling Speed
	mm	mm	mm	mm	°C	mm/sec
G12-3	0.5-0.6	6.8	16.0	5.1	1250	125
G12-4	0.5-0.6	3.2	8.9	4.3	1230	125
IM-1	0.5	3.75	10.1	2.9	1250	125
IM-2	0.5	1.5	5.7	2.8	1250	125
IM-3	0.5	1.5	5.6	3.4	1250	125
IM-4	0.5	1.5	5.5	2.9	1250	125

* All packs had 0.8-mm-thick tantalum interlayers and CaO parting agent between the preform and interlayers except IM-4 which used a CaF_2 release agent. Picture frames and covers of all packs were made from Ti-6Al-4V alloy.

6.3 Cold Rolling Procedures.

All cold rolling of direct cast strip was done at Texas Instruments, Materials and Controls Division in Attleboro, Massachusetts using their proprietary isobaric rolling technique (4). Because of the proprietary nature of the isobaric rolling process, detailed information about the techniques and procedures used to roll the direct cast strip was not available, but the rolled foils were all delivered to Ribtec for testing and evaluation.

CP-titanium. The direct cast CP-Ti was processed into foil in two rolling and annealing cycles: 1) initial breakdown from approximately 0.6mm gauge to 0.45 mm gauge followed by vacuum annealing at 700°C for two hours; 2) the strip was then rolled to final gauge, nominally 0.12-mm-thick and again vacuum annealed at 700°C for two hours.

Ti-1.2Al-0.8V Alloy. Two strips were cast from the Ti-1.2Al-0.8V alloy and designated Strip A and Strip B. Strip A was cast during a hearth tilt time of 3.4 seconds at a casting speed of 1.25 m/s on a water-cooled-molybdenum chill roll with a knurled surface. Strip B was cast during a hearth tilt time of 4.3 seconds at a casting speed of 1 m/s on a water-cooled-molybdenum chill roll with a peened surface.

Strip A was slit to 73-mm-wide and rolled to foil gauge in two rolling cycles: a 50% reduction from 0.38mm/0.48mm to 0.25mm then annealed at 700°C for 2 hours in vacuum and subsequently rolled to 0.13mm. Strip B was slit to 75-mm-wide and rolled from as-cast thickness of 0.4mm/0.5mm to 0.25 mm in one cycle. After rolling, both foils were vacuum annealed at 700°C for 2 hours.

Ti-6Al-2Sn-4Zr-2Mo Alloy. Three samples approximately 0.8-mm-thick were cold rolled to approximately 20 percent reduction and subsequently vacuum heat treated at 900°C for one hour. Following the heat treatment, samples were cold rolled to 0.15mm to 0.20mm gauge. Subsequently the material was vacuum heat treated at 900°C for one hour and rolled to the final 0.1mm gauge. Finally, the 0.1-mm-thick foil was vacuum annealed at 900°C for one hour.

Timetal-1100. The cast Timetal-1100 strip was rolled two times with one intermediate anneal at 871°C for 2 hours. After 16% cold reduction of the cast strip, vacuum annealing at 871°C for 2 hours and a further 22% cold reduction, cracks were found on both surfaces of the strip.

Ti-11Al-40Nb Alloy. Primary breakdown consisted 50 percent of cold work and intermediate vacuum annealing at 996°C for one hour followed by cold rolling to the gauge of approximately 0.125 mm. The same heat treatment cycle has been used for final anneal. In addition, a sample of direct cast strip (after a surface treatment) had been successfully cold rolled from approximately 0.7-mm-thickness to final gauge 0.125 mm without intermediate anneal. The cast strip material was total cold reduced approximately 82 percent.

6.4 Evaluation.

Chemical analyses were performed on the as-cast strip and cold rolled foils to determine the elemental composition and the interstitial content. All chemical analyses were performed by a commercial testing laboratory using the techniques as shown below:

Element	Technique
Oxygen, Nitrogen	Inert Gas Fusion
Carbon	Combustion
Hydrogen	Vacuum Hot Extraction
All others	Direct Coupled Plasma

The average surface roughness R_a and mean roughness depth R_z of the foils were

measured with a portable profilometer. The surface roughness values were an average of at least six traces with a traverse length of 5mm and an evaluation length of 4mm.

Dog-bone shaped tensile specimens 76-mm-long with a gage section 25mm x 6.4 mm were machined from the cold rolled foils. The specimens were instrumented with back-to-back extensometers with a 25 mm gage length and a total strain capacity of 50 percent. Tensile testing was performed in a universal testing machine with hydraulic grips, at a cross-head rate of 0.25mm/min up to a total strain of 2%. At 2% strain, the cross-head rate was increased to 1.25 mm/min. The extensometer strain values were averaged for each specimen. The data given for all the mechanical properties are the average of three tests for each foil and direction.

7.0 RESULTS AND DISCUSSION

7.1 Casting Results.

The effects of different process parameters on the cast strip were investigated. The parameters included: chill roll surface preparation; chill roll preheat temperature; tilting time; casting speed; and hearth standoff distance.

Chill Roll Surface. Five different chill roll surfaces were tested with the Ti-1.2Al-0.8V alloy: three different 60° diamond knurl patterns (25, 30 and 40 pitch); a mechanically peened surface (3M RotoPeen); and an electrochemically etched dot pattern. The average surface roughness (R_a) of each surface was measured in four positions 90° apart along the chill roll circumference with a portable profilometer.

The longest Ti-1.2Al-0.8V alloy titanium strips were cast on chill rolls with high R_a. The 25 pitch knurled surface exhibited the highest R_a at 6μm or greater and consistently cast the longest Ti-1.2 Al-0.8V alloy strips. Peening resulted in surface roughness approaching 5μm. All of the Ti-1.2 Al-0.8V alloy strips greater than 2-m-long were cast on the 25 pitch knurl or the Roto-peened surfaces. Inspection of the chill roll casting surface with a magnification of 25x revealed that both the 25 pitch knurl and peened surfaces had burrs or upset metal on the surface.

The R_a was progressively lower for the 30 pitch and 40 pitch knurled surfaces. Inspection of the chill roll casting surface with a magnification of 25x revealed that the 30 pitch and 40 pitch knurl patterns had no burrs or upset metal along the knurl. The lowest R_a of all chill roll surfaces was measured on the electrochemically-etched dot pattern. The etching system selectively removed metal from the chill roll surface through a stencil. Inspection of the chill roll casting surface with a 25x microscope revealed that the dots were chemically milled from the chill roll surface leaving the surface unchanged between the dots.

One theory to explain the effects of chill roll roughness on casting strip was that the liquid titanium adhered to the high points on the chill roll circumference. An irregular, rough casting surface increased the momentum transfer to the liquid and changed the wetting characteristics by disturbing the meniscus.

Chill Roll Pre-heat. A closed-loop hot water system was installed to test the effects of preheating the chill roll. During one experiment, the casting water temperature was 53°C and a 0.5-m-long strip was cast on the electrochemically etched surface. The surface was preheated to 66°C during a second experiment and a 0.4-m-long strip was cast. During a third experiment, the casting water temperature was 43°C and a 1.3-m-long strip was cast on the 30 pitch knurled surface. Next, the chill roll was preheated to 66°C and a 0.8-m-long strip was cast. Based on the results of these four experiments, we concluded that the preheat of the chill roll did not improve the wetting characteristics for Ti-1.2Al-0.8V alloy based on the length of strip cast.

Casting Speed. Titanium alloy strips were cast at speeds within the range of 0.75 m/s to 1.5 m/s. At casting speeds below 0.75 m/s, the liquid titanium did not wet the chill roll surface resulting in little or no strip being cast. At casting speeds above 1.5 m/s, the strip quality was unacceptable: either holes, uneven surfaces, narrow widths or longitudinal cracking occurred.

Hearth Tilt Time. All of the titanium alloys were melted in a water-cooled copper hearth in a nearly horizontal position. Strip was cast when the hearth was tilted about the same axis of rotation as the chill roll to a position of 45° above horizontal. Tilting times as low as 2.8 seconds and as high as 5.8 seconds were investigated. In general, casting at low tilting times resulted in thicker, shorter strips while casting at longer tilting times resulted in longer, thinner strips.

Hearth Standoff. The hearth standoff was an important variable in casting. Standoff distances as low as 0.3 mm and as high as 1.5 mm were tested. In general, greater standoff distances resulted in smoother, more uniform cast strip.

Hearth Design. Three experiments were performed with a two-part hearth consisting of a water-cooled copper crucible that was hinged against a stationary lip or spout. The stationary lip was filled with liquid titanium by the tilting crucible. The liquid overflowed the lip onto the circumference of the rotating molybdenum chill roll.

One experiment was performed with a stationary lip positioned at the horizontal centerline of the chill roll. The crucible rotation angle was 45°. The liquid metal flooded the lip during the 6 second tilt time with titanium flowing over the sides of the lip as well as onto the chill roll. No useful strip was cast.

Two experiments were performed with a stationary lip positioned at 30° above the horizontal axis of the chill roll. The crucible rotation was limited b 20° during a 3 second tilt time. The first experiment resulted in a 2-m-long strip. There were lumps and folds along the length of the strip. The lumps on the strip appeared to have first solidified against the lip, broke off and were carried off with the strip. The standoff distance between the lip and chill roll was increased from 1 mm to 1.4mm during the next experiment and the number of lumps decreased but so did the strip length.

Vapor Deposits. The cast Ti-aluminide strips were covered by a thin dust which also coated the inner surfaces of the process vessel and was believed to be condensate from a vapor cloud during melting of alloys with high aluminum content. It was determined that this dust was an oxide of Ti and Al, as would be expected. Visibility was poor during plasma arc melting of γ Ti-aluminide due to the dense vapor cloud that condensed on the inner surfaces of the chamber and viewports. The melting times were shorter for γ Ti-aluminide because the condensate on the viewports made them opaque and the operator could not see the liquid titanium alloy in the hearth after melting for approximately 8 min. A magnetically-actuated wiper was fabricated to clean the operator's viewport and extend the melting and casting time

by 3 to 4 minutes. As a result of the shorter melting times. the volume and the temperature of the liquid γ Ti-aluminide was lower than other titanium alloys which were typically melted for 14 minutes.

Design of Experiments. A matrix of sixteen experiments with four independent variables was constructed to test the effects of process variables on strip quality. The cast strips were assigned values on a scale from a low of 0 to a high of 5 according to an estimation of the length of rollable strip obtained from each strip. The four factors and their limits were defined as follows:

Parameter	UCL	LCL
Casting speed (m/s)	1.0	0.8
Arc Current (amperes)	550	500
Hearth standoff (mm)	1.5	0.6
Hearth tilt time (sec)	4	3

Key: UCL = upper control limit; LCL = lower control limit.

The matrix and responses were entered into a computer software package called X-Stat version 2.0. The quality response data were fit to a quadratic regression model. The standoff distance between the hearth and the chill roll was the most important variable affecting cast strip quality according to the quadratic regression model.

Based on the quadratic regression model, strip quality would be maximized under the following conditions:

Casting speed	0.8 m/s
Arc current	550 amperes
Hearth standoff	1 mm
Hearth tilt time	3.6 seconds

Three experiments were performed under the above experimental conditions. The strip produced during the first experiment caught up on the conveyor and did not produce any flat strip. The second experiment resulted in strip with a quality level of 1. It was observed that the chill roll surface was relatively smooth after the second experiment. The chill roll surface was peened lightly and a third experiment was performed under the same conditions: the quality level of the strip improved to 3.

Clearly, there were factors other than casting speed, arc current, hearth standoff, and hearth tilt time that affect the cast strip quality. Obviously the chill roll surface preparation is one factor that affects strip quality that we have not been able to quantify to date.

Summary - A total of 122 casting experiments were conducted with 6 different alloys. Table 7.1 illustrates what was observed to be optimal operating parameters for each particular alloy.

Table 7.1: Observed Optimal Melting and Casting Parameters

Alloy	Chill Roll Surface	Hearth Standoff (mm)	Casting Speed (m/s)	Tilt Time (sec)	Mean Voltage (v)	Mean Current (a)
CP - Ti (CP-46)	25 tpi knurl	1.5	1.00	3.5	140	506
Ti-1.25Al-0.8V (CP-17)	25 tpi knurl	0.66	1.25	3.4	130	507
Ti-6Al-2Sn-4Zr-2Mo (6242-2)	Roto-Peen	1.5	1.00	3.5	157	480
TiMetal-1100 (1100-7)	Roto-Peen	1.5	1.00	3.1	143	527
Ti-11Al-40Nb (Orth-7)	Roto-Peen	1.5	1.00	3.1	145	523
Ti-31Al-5Nb-3Cr (G-12)	Roto-Peen	0.9	1.00	4.5	138	536

CP Titanium. Eleven experiments were performed to cast CP-Ti on a molybdenum chill roll. CP-Ti strip was cast on a 25 pitch knurled surface but did not cast on the RotoPeen surface. It is not known why 98% pure Ti (Ti-1.2Al-0.8V alloy) cast on the RotoPeen surface while >99% pure titanium did not.

Ti-1.2Al-0.8V alloy. It was estimated that approximately 20% Ti-6Al-4V alloy scrap was melted with CP titanium scrap to form the resulting Ti-1.25Al-0.8V alloy. The alloying was unintentional and was not discovered until the alloy strip had been cast, cold rolled and evaluated.

Two different strips of a Ti-1.25 Al-0.8V alloy, designated Strips A and B, were cold rolled to foil gauge. Strip A was 3.5-m-long with an average width of 97mm. Strip A was cast on a knurled chill roll surface. The as-cast microstructure contained acicular alpha,

serrated alpha and beta phases (Figure 7.1). The cast strip was fully dense with no porosity or cracks. Irregularities in the rough free cast surface can be seen. Strip B was 3.2-m-long with an average width of 96mm. Strip B was cast on a peened chill roll surface.

Figure 7.1: Optical micrograph of as-cast strip A.

Timetal-1100. Twenty four experiments were performed to cast Timetal-1100 alloy. All of the as-cast strips exhibited micro-cracking on the chill-cast surface and solidification-induced porosity on the free cast surface. Two cast strips, designated 1100-5 and 1100-7 were cold rolled.

Intergranular cracks were found on the chill-cast surface of the as-cast Timetal-1100 alloy strip (ID# 1100-5) between prior beta grains (Figure 7.2a). The cracking probably occurred at temperatures above the beta transus (approximately 1016°C for Timetal-1100). During cooling, the beta transformed to acicular alpha which can be seen inside the prior beta grains.

On the free-cast surface of the as-cast Timetal-1100 strip, surface porosity was evident (Figure 7.2b). The voids appeared to be a result of solidification: as the solidifying strip emerged from the liquid pool there was a deficiency of liquid to fill the cavities formed after solidification of the primary grains.

The carbon and gas content of the Timetal-1100 cast strips that were later cold rolled were measured and are shown in Table 7.2. The levels of carbon and gasses in the as-cast strips were all lower than the chemical composition limits specified for Timetal-1100; i.e., oxygen: 900ppm max; nitrogen: 300ppm max; and carbon: 400ppm max.. It is unlikely that carbon or gases contributed to the micro-cracking observed in the cast strip.

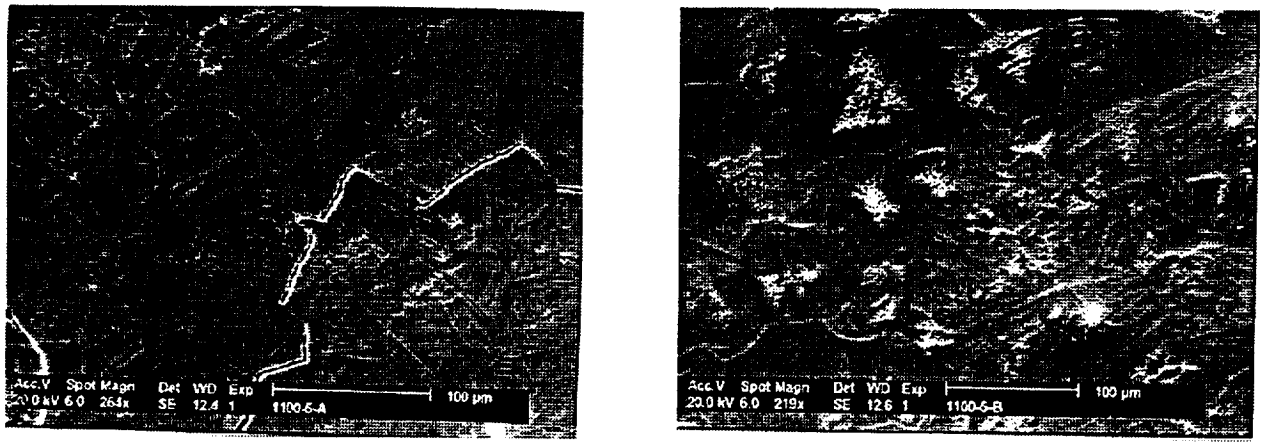

a b

Figure 7.2: SEM micrographs of as-cast Timetal-1100 strip illustrating (a) microcracks on chill cast surface; and (b) voids on free cast surface.

Table 7.2 Carbon and Gas Content of Timetal-1100 Cast Strip (wt ppm)

Sample ID	C	O	H	N
1100-1	100	783	45	15
1100-5	100	829	48	63
1100-7	100	761	52	45

Longitudinal grooves were found on the Ti-1100 strip cast on either knurled or peened chill roll surfaces. The grooves on the strip corresponded to "peaks" in the skull that solidified in the pouring spout. The grooves on the strip were eliminated by increasing the hearth standoff distance from 0.6 mm to 1.5 mm.

In an effort to reduce micro-cracking in Timetal-1100 strip, one experiment was conducted to cast the alloy on a smooth molybdenum chill roll at 1.1 m/s casting speed with a mean plasma arc power of 59kW. It was postulated that if the cracking was related to residual stresses from thermal contraction, the strip would be less likely to adhere to a smooth chill roll surface. By increasing the casting speed, the contact time with the chill roll was decreased. By reducing the plasma arc power, the superheat of the liquid titanium would be lower, therefore the thermal gradient would be lower. Collectively, these three parameters did not affect cracking of the cast strip, however. The experiment was repeated with a molybdenum chill roll with a knurled (25 pitch) casting surface and again, microcracks were found on the strip surfaces.

Ti-6Al-2Sn-4Zr-2Mo alloy. Five experiments were performed to cast Ti -6242 alloy strip from scrap on a Roto Peened molybdenum chill roll. The strip cast extremely well, with no evidence of microcracks on the strip surfaces.

The surfaces of cast strips of Ti-6242 alloy were examined in the SEM. The free-cast surface exhibited intergranular porosity related to solidification of the strip: primary solidification depleted the liquid which resulted in voids between the primary grains, Figure 7.3a. No cracks were found on the chill cast surface, Figure 7.3b.

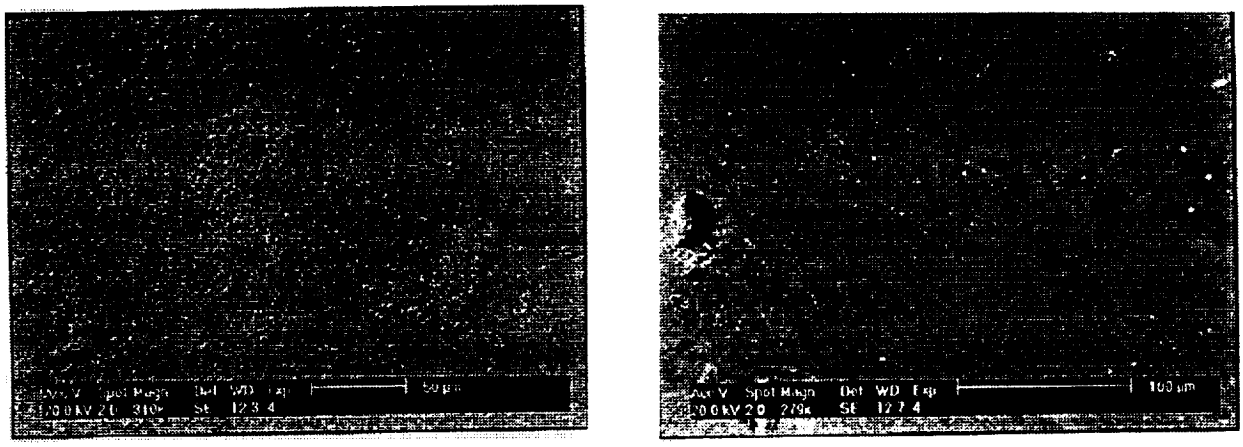

a b

Figure 7.3: Scanning Electron Micrographs of (a) free-cast surface and (b) chill cast surface of as-cast Ti-6242 alloy strip.

Ti-11Al-40Nb Alloy. Certified ingots of Ti-11Al-40Nb alloy were remelted in the plasma melt overflow furnace and cast into strip on a molybdenum chill roll. Two strips were cast on a 25 pitch knurled surface: the remaining thirteen strips were cast on a RotoPeen surface.

The Ti-11Al-40Nb alloy required high power to melt (in the range of 70 kW to 75 kW). It appeared that the volume of liquid melted in the hearth was smaller than CP-Ti and the liquid appeared to have less superheat. Vaporization was significant, but less than γ Ti-aluminide, and did not limit the melting time.

The chemical composition of the as-cast orthorhombic strip was measured using a DC Plasma technique and is presented in the Table 7.3. Strip O-5 was the first remelt of a skull using ingot 3B0726 and strip O-11 was the sixth remelt from that skull. Strip O-7 was the third remelt of a skull using ingot 3B0724. "Start" and "end" designate the position on the strip the samples were taken from. There appeared to be a slight loss of aluminum and niobium during plasma arc melting.

The carbon and gas contents of the as-cast strips and ingot feedstock were measured

and are presented in Table 7.4. Strips O-1, O-2 and O-3 were cast from ingot 3B0723, strips O-5 and O-11 were cast from ingot 3B0726 and strip O-7 was cast from ingot 3B0724. In the worst cases, the oxygen content increased by roughly 100 wppm but in all orthorhombic Ti-aluminide samples, the oxygen content was less than 1000ppm.

Table 7.3. Chemical Composition of Orthorhombic Ti-Aluminide Ingots and Strips

	Al		Nb		Fe	
Sample ID	wt %	at %	wt %	at %	wt %	at %
Ingot 3B0726	11.4	22.7	40.3	23.3	0.086	0.082
Strip O-5 start	11.1	22.0	39.6	22.9	0.111	0.106
Strip O-11 end	11.1	22.1	39.9	23.0	0.089	0.085
Ingot 3B0724	11.1	22.0	39.4	22.7	0.088	0.084
Strip O-7 Start	10.9	21.7	39.7	22.9	0.089	0.085

Table 7.4. Carbon and Gas Content of Ti-11Al-40Nb Alloy (wppm)

	C	O	H	N
Ingot 3B0723	100	916	28	123
Strip O-1	100	861	24	166
Strip O-2	140	914	34	194
Strip O-3	100	932	34	179
Ingot 3B0726	100	854	24	138
Strip O-5 start	100	974	23	158
Strip O-11 end	100	877	42	140
Ingot 3B0724	100	805	19	123
Strip O-7 end	100	910	38	138

X-ray diffraction (XRD) revealed the as-cast microstructure consisted of a single phase: the ordered beta phase with a B2 structure. This finding was confirmed by transmission electron microscopy (TEM). Foils for TEM were thinned from the free cast surface of cast strip O-5. Figure 7.4a shows a bright field TEM micrograph of two grains. The crystal structure of both grains was B2, as evidenced by the [001], [011] and [111] zone axis select area electron diffraction patterns (Figure 7.4b - 7.4d).

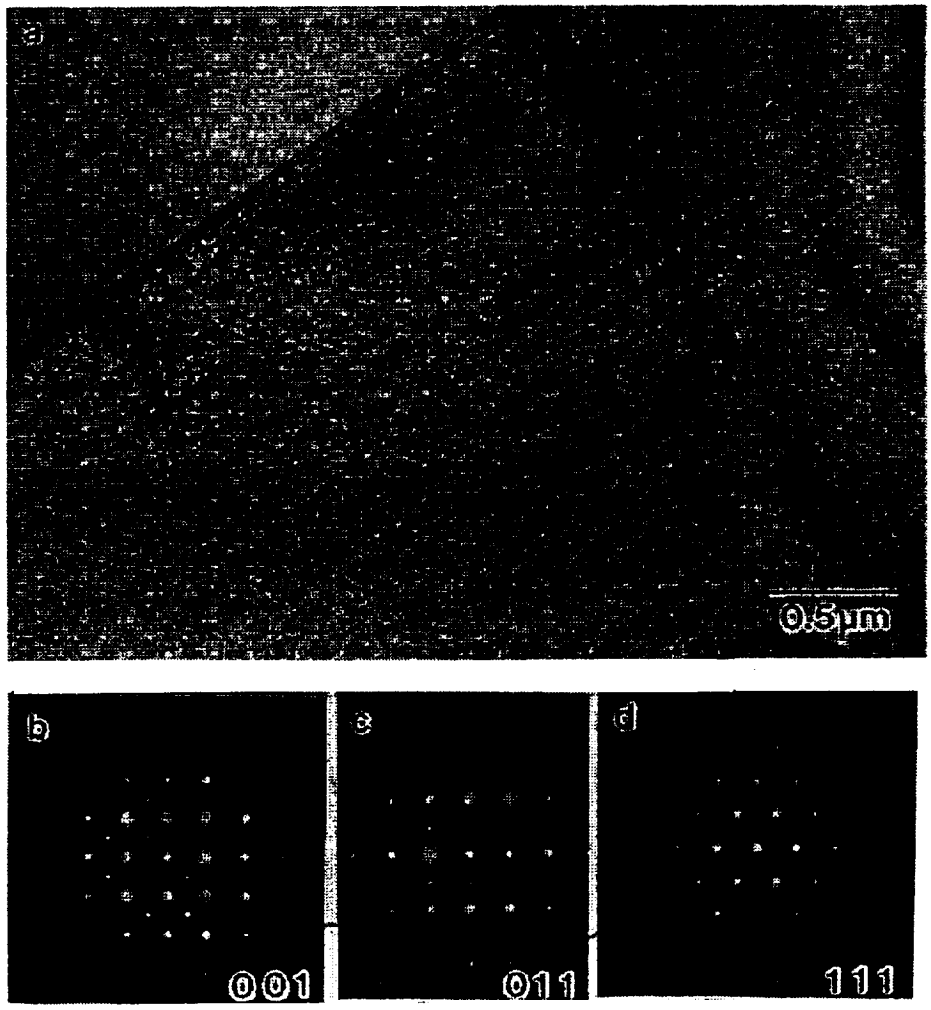

Figure 7.4. (a) Bright-field TEM micrograph and (b-d) select area electron diffraction patterns (SADP) taken from Ti-11Al-40Nb alloy strip O-5.

SEM micrographs of the as-cast surfaces of strip O-9 are shown in Figure 7. 5. Both the chill cast surface and free cast surface exhibited equiaxed grains. The diameter of the grains was approximately 50 μm. The free surface exhibited a dendritic structure while the chill cast surface exhibited fully transformed grains.

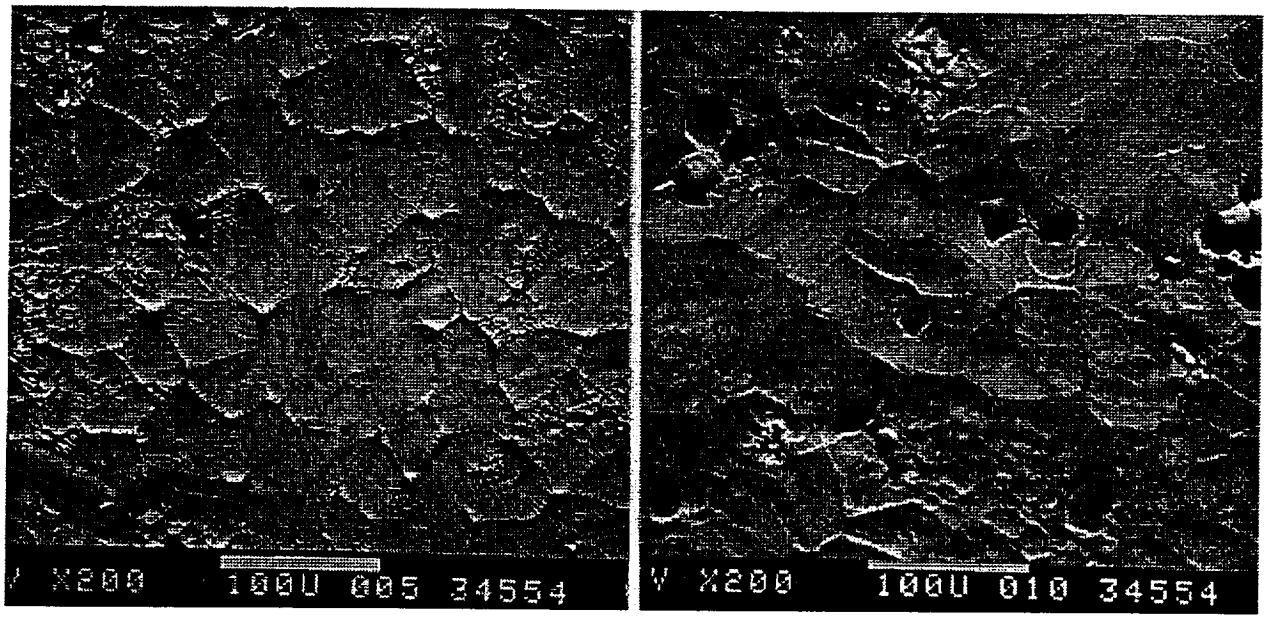

a b

Figure 7.5: SEM micrographs of as-cast Ti-11Al-40Nb strip material: (a) free surface; (b) roll side surface.

Ti-31Al-5Nb-3Cr Alloy. Fourteen experiments were conducted to melt and cast γ-based alloy strip. Six of the experiments successfully resulted in cast strip. During the first two experiments, the γ alloy skull from the Phase I research project was used as feedstock. One 3.3-m-long strip was cast at a rate of 1 m/s on a 25 pitch knurled molybdenum chill roll with a 4.3 second tilt time and a hearth to chill roll standoff of 0.4mm during experiment G2. The cast γ alloy strip G2 was so brittle that it cracked during handling.

Experiments G5 and G6 resulted in cast strips, each cast on a 25 pitch knurled molybdenum chill roll at a rate of 1 m/s with a 4.4 second tilt time and hearth to chill roll standoff distances of 0.4mm and 0.5mm, respectively. In both experiments, the overall length of strip corresponded to one revolution of the chill roll 0.7 m.. The standoff distance between the pouring spout and the chill roll was increased from 0.5mm to 0.9mm during experiments G12 and G13 and further increased to 1.5mm during experiment G14. The longest γ strip was cast during experiment G12. The chill roll jammed during experiment G13 while casting strip. Relatively brittle strip was cast during experiment G14. Samples of Ti-31Al-5Nb-3Cr

alloy direct cast strip from experiment G12 were delivered to Wright Laboratory for heat treatment, microstructural evaluation and hot pack rolling.

Chemical Analysis. The aluminum, niobium and chromium content of the γ Ti-aluminide ingots and strips cast from them were measured using a DC Plasma technique and are presented in Table 7.5.

Table 7.5: Chemical Composition of γ Ti-Aluminide Ingots and Strip

	Al		Nb		Cr	
Sample ID	wt %	at %	wt %	at %	wt %	at %
Ingot 3B0719	30.8	45.0	4.7	2.0	2.5	1.9
Strip G5	30.7	44.8	4.6	2.0	2.5	1.9
Strip G6	30.7	44.8	4.6	2.0	2.5	1.9
Strip G12	30.8	45.0	4.7	2.0	2.6	2.0
Ingot 3B0718	31.2	45.5	4.7	2.0	2.7	2.1
Strip G13	30.9	45.1	4.7	2.0	2.7	2.1

The loss of aluminum during remelting of the ingots was 0.3 wt% or less which was considered low given that the skulls were remelted several times. Strips G5 and G6 were the third and fourth remelts, respectively, from a skull using ingot 3B0719. Strip G12 was the third remelt of a different skull using ingot 3B0719. Strip G13 was the first remelt from ingot 3B0718. Despite the very heavy vapor deposit that was observed during melting γ-based alloys, there appeared to be very little alloy loss after plasma arc melting. It should also be noted that the aluminum content of the induction-melted ingots was lower than the target of 46 atomic percent.

Carbon and Gas Analysis. The carbon, oxygen, nitrogen and hydrogen content of the γ-based alloy ingots, plasma arc melted skulls and cast strips are presented in Table 7.6.

The γ alloy skull that remained from the Phase I research project was used during the first two experiments to cast γ strip in this project. The brittleness of strip G2 can be attributed to the 1400 ppm oxygen content of the skull from which it was cast. The strips identified as G5, G6, G12, G13 and G14 were cast from the induction melted γ alloy ingots described in the previous section of this report. Oxygen, hydrogen and nitrogen levels increased modestly during plasma arc skull remelting and strip casting: all cast strip samples had acceptably low gas content. There was no measurable increase in carbon content after melting and casting

γ Ti-aluminide. Furthermore, creep flattening of strip G12 did not increase the carbon or gas content of the cast strip.

Table 7.6: Carbon and Gas Content of γ Ti-aluminide Ingots and Strip

	C	O	H	N
γ Skull (Phase I)	200	1421	n/a	108
Ingot 3B0719	100	521	27	59
Strip G5	100	523	27	82
Strip G6	100	546	26	96
Strip G12 (Beginning)	100	519	30	74
Strip G12 (End)	100	604	21	91
Strip G12 (Creep Flat)	100	556	34	94
Ingot 3B0718	100	568	27	100
Strip G13 (Beginning)	100	602	24	114
Strip G13 (End)	100	572	26	122
Strip G14 (End)	100	647	30	99

Cast Microstructure. The microstructure of strip G12 was similar in both the leading and trailing ends; it comprised a mixture of feathery massive γ and patches of very fine lamellar microstructure (Figure 7.6). Bright field micrographs (Figure 7.7) also revealed a noticeable amount of porosity, most of it being found on the surface or interconnected to that surface.

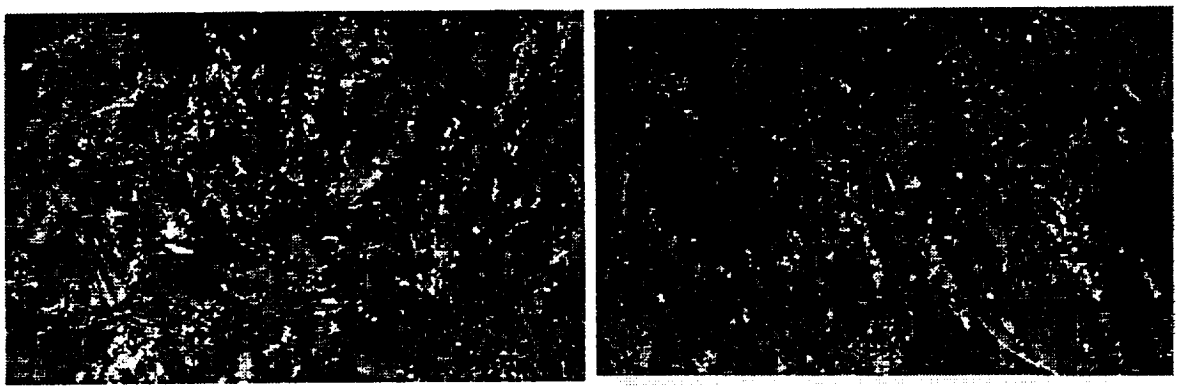

Figure 7.6: Micrographs of (a) the leading end and (b) the trailing end of as-cast Ti-30.8Al-4.7Nb-2.6Cr strip G12: polarized light (200x).

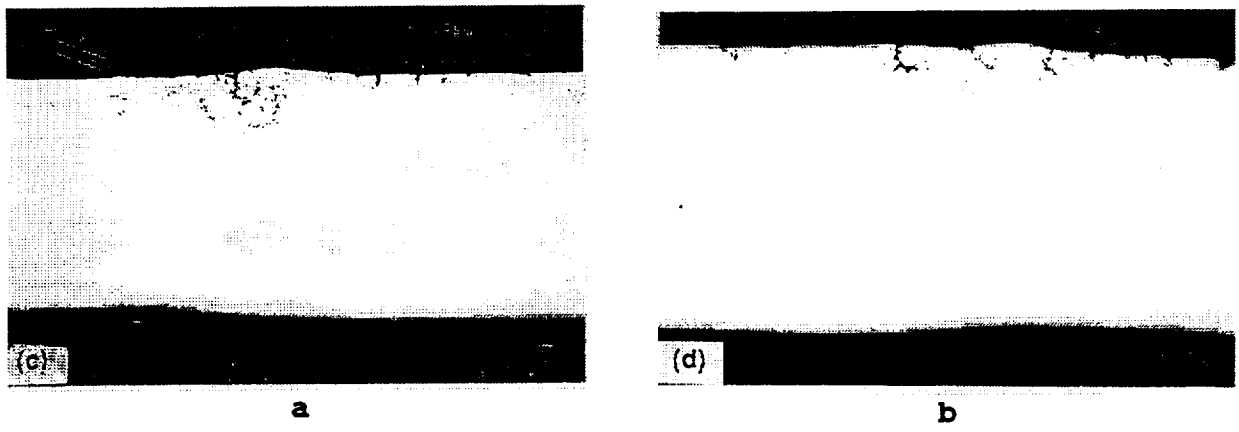

Figure 7.7: Micrographs of (a) the leading end and (b) the trailing end of as-cast Ti-30.8Al-4.7Nb-2.6Cr strip G12: as-polished, bright field (100x).

7.2 Pack Rolling Results.

Thermal treatments. Heat treatment at 1232°C led to small changes compared to the as-cast structure as shown in Figure 7.8. The lamellar colony size appeared to be smaller, and nearly-equiaxed features (probably γ grains) appeared to have nucleated and grown from the prior regions of feathery, massive γ.

Heat treatment at 1277°C, a temperature only 22°C below the nominal alpha transus, led to a nearly fully lamellar microstructure with a small amount of equiaxed γ in the leading end sample (Figure 7.9a) and a structure with approximately two-thirds lamellar structure and one-third γ in the trailing end sample (Figure 7.9b). The morphology of the lamellar structure in samples heat treated at 1277°C suggested that such colonies were single phase alpha at the heat treatment temperature. The variation in the percentage of lamellar structure and in the size of the colonies between the leading and trailing end samples in this case can be explained by macro segregation (of the order of 0.5 atomic percent aluminum) which would give rise to a higher alpha transus for the material in the trailing end.

Heat treatment at 1343°C gave rise to microstructures which were almost totally feathery, massive γ, (Figure 7.10) consistent with the structure obtained by rapidly cooling Ti-31Al-5Nb-3Cr alloy from the single-phase alpha field. Even though the samples were air cooled in the heat treatment study, the thin cross-section of the material resulted in a relatively high cooling rate.

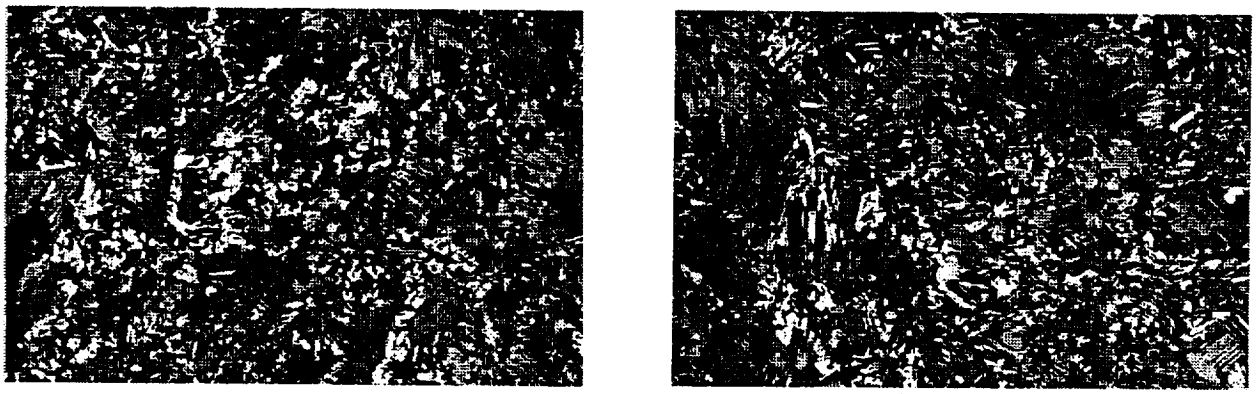

Figure 7.8: Polarized light optical microstructures (200x) of Ti-30.8Al-4.7Nb-2.6Cr direct cast strip G12 after one hour heat treatment at 1232°C ; (a) leading end (b) trailing end.

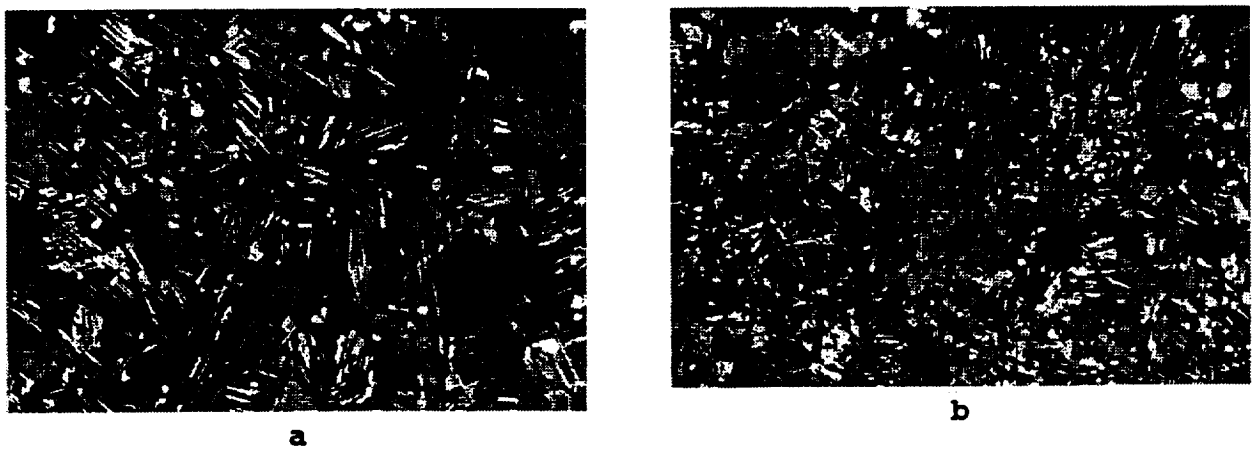

Figure 7.9: Polarized light optical microstructures (200x) of direct cast strip G12 after one hour heat treatment at 1277°C; (a) leading end (b) trailing end.

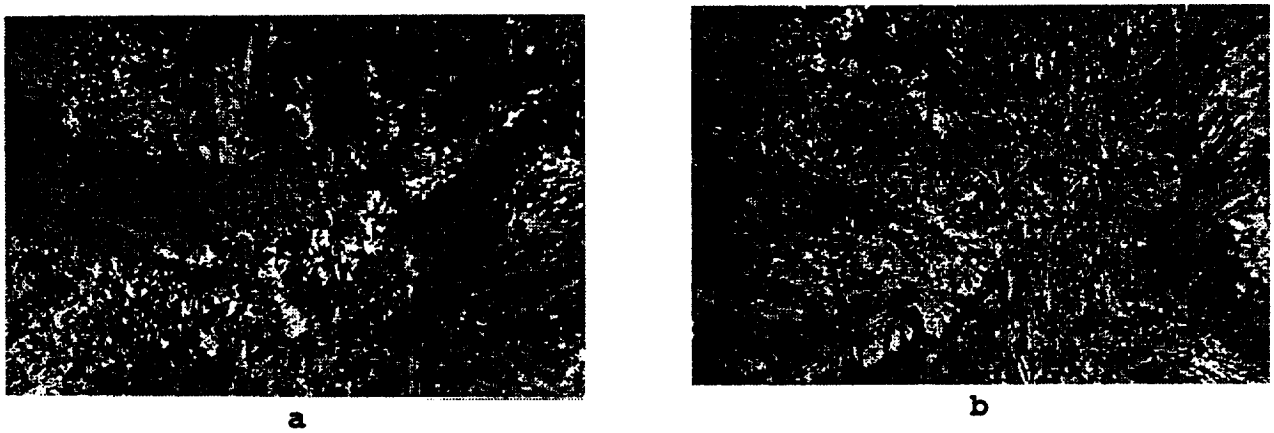

Figure 7.10: Polarized light optical microstructures (200x) of direct cast strip G12 after one hour heat treatment at 1343°C ; (a) leading end (b) trailing end.

Hot Pack Rolling. The two trials to hot pack-roll direct cast Ti-30.8Al-4.7Nb-2.6Cr alloy strip were both unsuccessful. Preform G12-3 was rolled first. A section of the pack rolled at 1250°C taken after an overall reduction of approximately 70 percent is shown in Figure 7.11a. The γ preform was fractured while the tantalum interlayers were necked and fractured in various locations. The thickness of the γ workpiece based on both the macrograph (Figure 7.11a) and a micrograph (Figure 7.11b) was approximately 0.4 mm. Thus, a small amount of reduction was imposed on the cast γ preform, although it was much less than the overall pack reduction. The micrograph (Figure 7.11b) also suggested a rather brittle, tensile-type failure with little plastic flow. The microstructure did reveal, however, that hot working was indeed done high in the two-phase (α2 + γ) field, as desired.

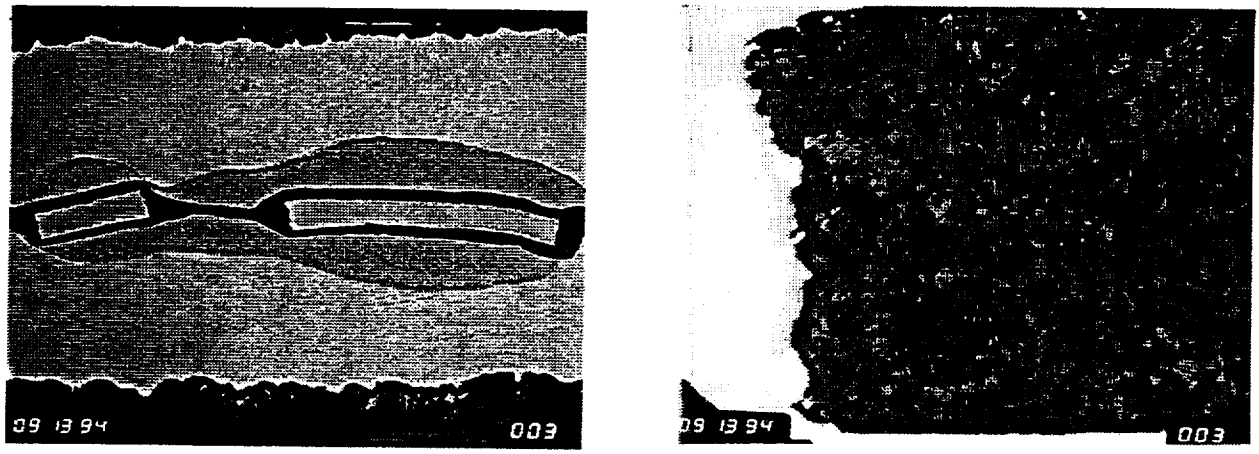

a b

Figure 7.11: Macrograph (a) and micrograph (b) of as-rolled, direct cast preform G12-3. In both photographs, the rolling direction is horizontal, and the thickness direction is vertical. Magnifications: (a) 16x, (b) 200x.

The second attempt at hot pack rolling (Preform G12-4) was conducted at 1230°C in an attempt to develop a finer, more ductile microstructure. Furthermore, the pack covers were made thinner (Table 6.1) in order to reduce the level of secondary tensile stresses in the γ preform. These stresses were induced by rolling a harder material in a softer can. Despite these changes, the γ preform still failed in a relatively brittle mode (Figure 7.12a,b), again undergoing a thickness reduction much less than the overall pack reduction. A macrograph (7.12a) and a micrograph (Figure 7.12c) of the failed sample showed evidence of substantial porosity on one of the two plan surfaces. The surface porosity in the preform may have contributed to the failure.

Because of the lack of success in hot pack rolling the direct cast Ti-30.8Al-4.7Nb-2.6Cr alloy strip, two wrought and recrystallized ingot metallurgy (IM) Ti-31.2Al-4.7Nb-2.7Cr preforms were cut from an isothermal forging for hot pack rolling. By this means, the importance of can design versus the structure and integrity of the γ preform on rolling performance was assessed. In the first two rolling trials conducted at 1250°C, the IM preforms fractured into many small pieces.

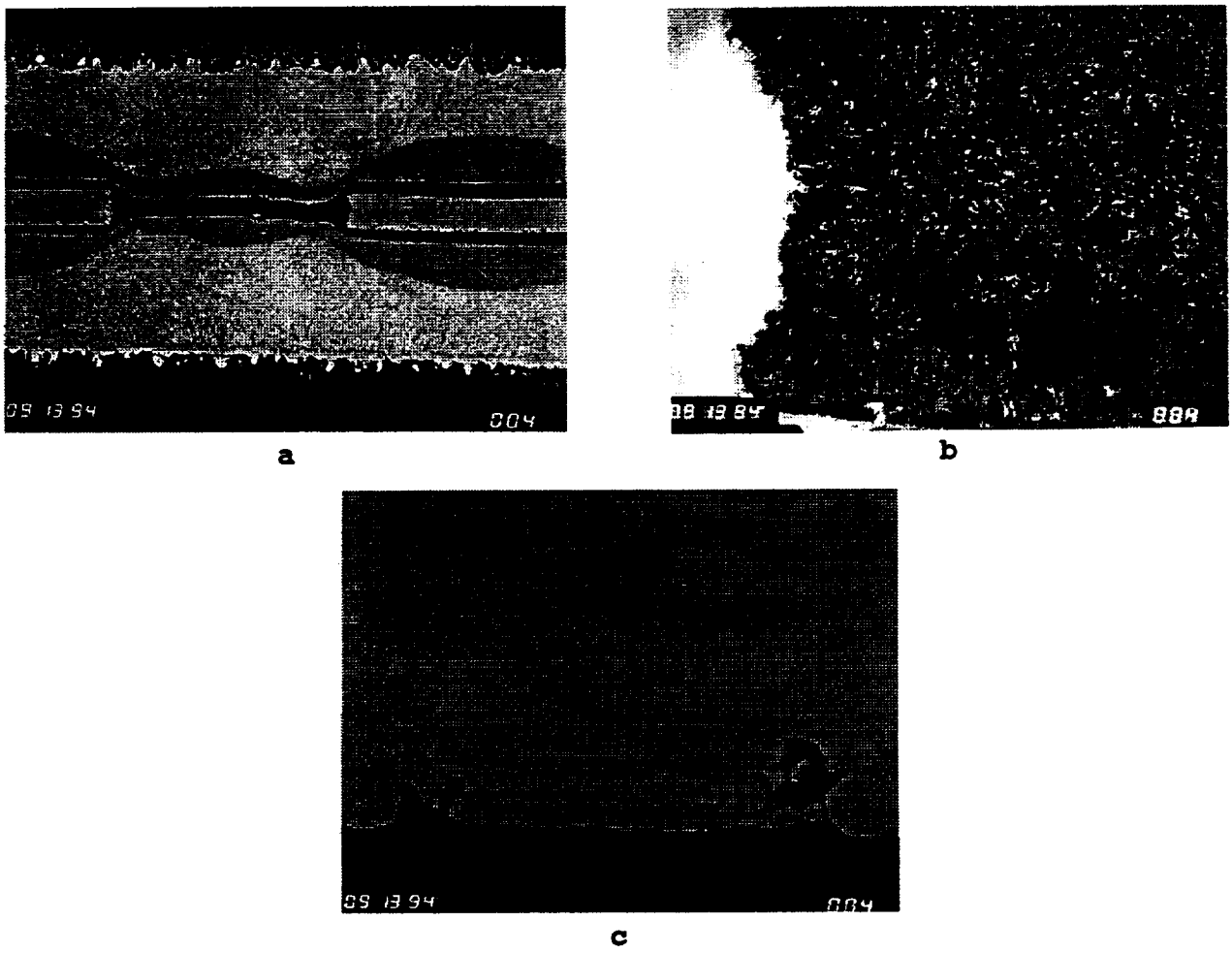

Figure 7.12: (a) Macrograph and (b,c) micrographs of as-rolled, direct cast preform G12-4. In all three photographs, the rolling direction is horizontal, and the thickness direction is vertical. Magnification: (a) 16x, (b) 200x, (c) 500x.

It was not possible to pinpoint the exact source of the failures in the first two pack-rolled wrought γ Ti-aluminide preforms; however, metallography on several of the broken pieces revealed one possible explanation for the poor rolling behavior. Micrographs (such as that in Figure 7.13) showed that the samples contained zones of coarse grains on both free surfaces. It was not clear whether these coarse-grain regions were (1) the remnants of the EDM recast layer, (2) a recrystallization product introduced by heating the cold worked (lapped) surfaces of the preforms, or (3) a reaction product between the γ Ti-aluminide preform and the calcium oxide parting agent. In any case, the surface layers appeared to be regions in which cracks nucleated and then propagated through the thickness.

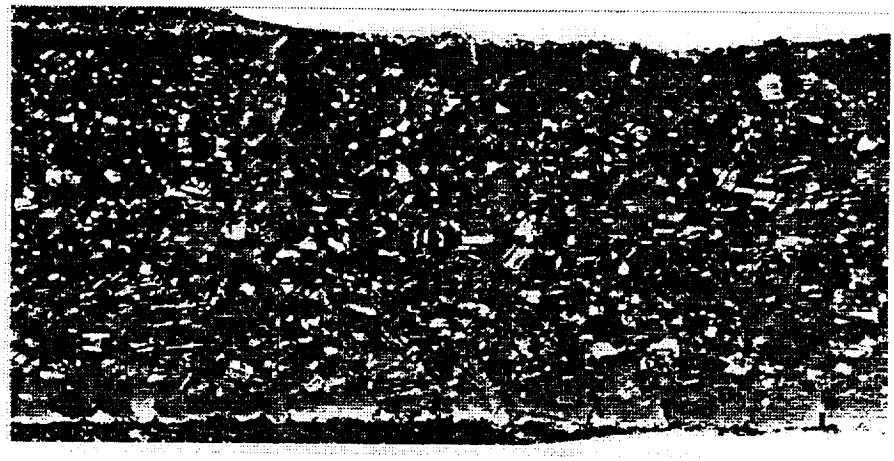

Figure 7.13: Polarized light, optical microstructure developed in forged-and-recrystallization-heat-treated Ti-31.2Al-4.7Nb-2.7Cr after hot pack rolling at 1250°C. Note the development of numerous superficial cracks and one larger thickness-direction crack. The rolling direction is horizontal, and thickness direction is vertical. (100x)

In the final attempt to establish the effect of surface condition on rollability, two additional 0.50-mm-thick preforms of wrought Ti-31.2Al-4.7Nb-2.7Cr were machined, canned, and rolled at 1250°C. In both cases, sufficient stock was ground from the EDM'ed plan surfaces to ensure complete removal of the recast layer. In one can, CaO was used as a parting agent, and in the other CaF_2 was used. The latter parting agent was selected to prevent oxygen contamination and possible losses in workability due to such effects.

The pack with the CaO parting agent was rolled to a 40 percent reduction in thickness. After slow cooling from the rolling temperature, the pack was cut open, and the γ preform was found to have fractured into a large number of small fragments as in previous trials.

The pack with the CaF_2 parting agent was rolled to an overall reduction of approximately 45 percent, slow cooled, and cut open. Although the preform in this case was cracked (Figure 7.14), its fracture appearance was totally different from that in previous trials. Specifically, there were relatively few cracks, and the geometry of the cracks suggested that the majority of the failures occurred during cool down and de-canning rather than during rolling. This hypothesis was supported by the fact that radiographs taken prior to decanning revealed only the transverse direction crack near one end of the workpiece. Equally important, the microstructure of the rolled piece was rather homogeneous. There was no evidence of coarse grains or flaws at the surfaces (Figure 7.15).

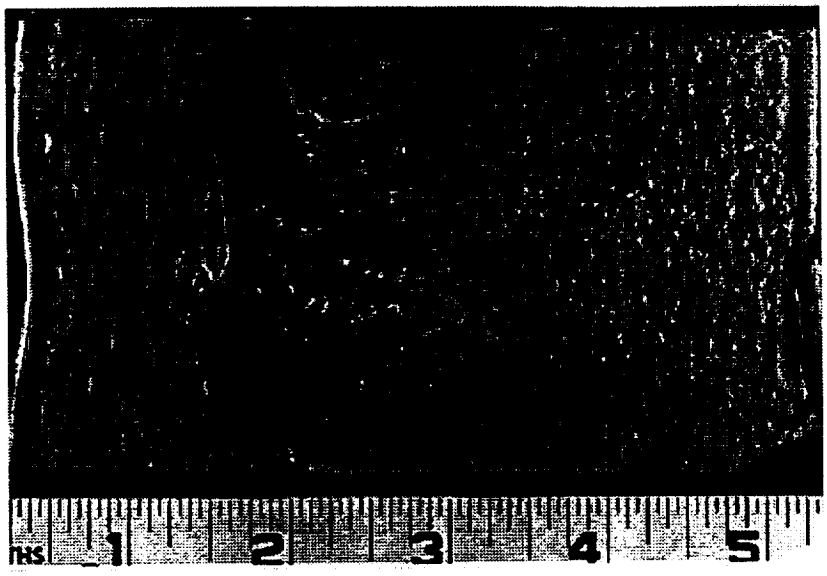

Figure 7.14: Macrograph of decanned sample IM-4 pack rolled using a CaF_2 parting agent.

Figure 7.15: As-rolled microstructure of sample IM-4 pack rolled using a CaF_2 parting agent. The rolling direction is horizontal, and the thickness direction is vertical. (160x)

7.3 Cold Rolling Results.

CP Titanium. The microstructure of the CP-Ti foils consisted of fine-grained, equiaxed alpha as shown in Figure 7.16. The grain size of the direct cast and cold rolled foils was smaller than No. 9 using the ASTM E-112 standard test procedure.

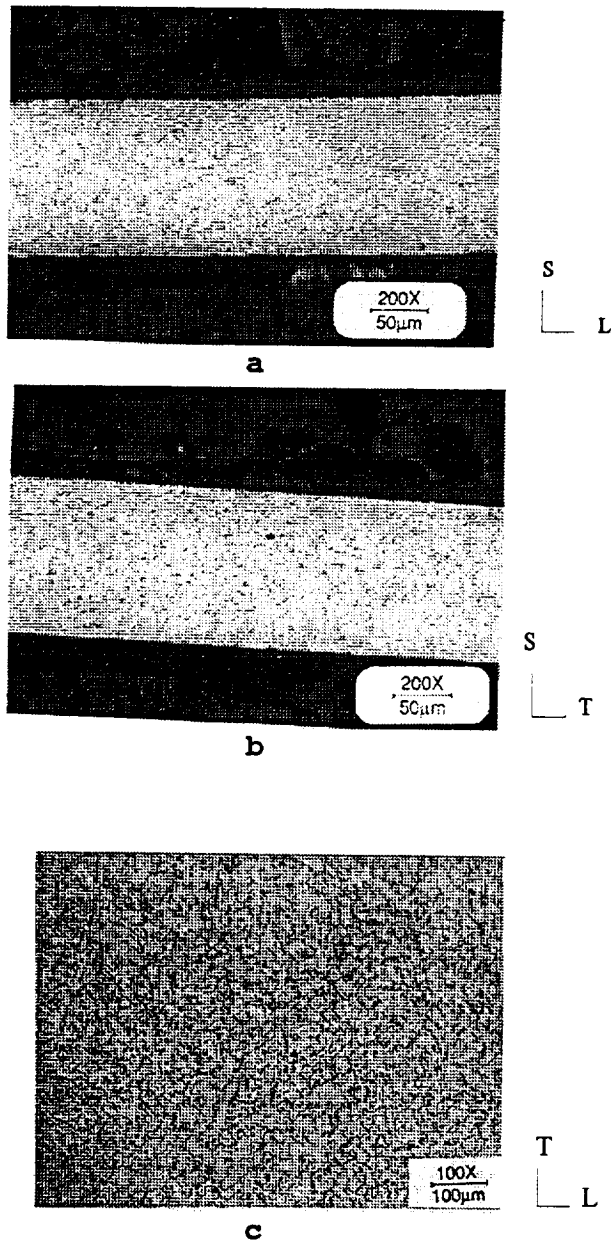

Figure 7.16. Optical micrographs of 0.125-mm-thick cold rolled and vacuum annealed direct cast CP-Ti foil showing fine, equiaxed microstructure: (a) Rolling direction; (b) Transverse direction; (c) In-plane

The carbon and gas content of the ingot metallurgy CP-Ti foil and of the as-cast CP-Ti strip and foil are presented in Table 7.7. The most significant difference between the ingot metallurgy (IM) and direct cast (DC) CP-Ti was the IM foil had one and a half times higher oxygen than the cast material. Cold rolling the cast strip resulted in higher carbon but lower gas content. The carbon content may have increased because of the lubricants used in cold rolling while the gas content may have decreased because of vacuum annealing.

The chemical compositions of ingot metallurgy and direct cast CP-Ti strip and foils are presented in Table 7.8. The chemical compositions of the IM and DC strip and foils were comparable.

Table 7.7. Carbon and Gas content of CP-Ti strip and foils (wt ppm)

Element	IM/CR foil	As-cast strip	DC/CR foil
Carbon	380	130	220
Oxygen	1960	1260	1210
Nitrogen	130	110	80
Hydrogen	57	31	8

Key: IM = ingot metallurgy; DC = direct cast; CR = cold rolledand annealed

Table 7.8. Chemical composition of CP-Ti Strip and Foils (wt %)

Element	IM/CR foil	As-cast strip	DC/CR foil
Titanium	99.5	99.6	99.3
Iron	0.12	0.045	n/a
Manganese	<0.003	0.018	n/a
Aluminum	0.043	0.069	0.079
Vanadium	0.008	0.030	0.018

Key: IM = ingot metallurgy; DC = direct cast; CR = cold rolled and annealed

The tensile properties of the direct cast and cold rolled CP-Ti strip were measured and are presented in Table 7.9. The IM foils had 8% higher strength than the DC foils, which might have resulted from the higher oxygen content. The total elongation of the IM foils was 60% greater than the DC foils while Young's modulus for the DC foils was 20% greater than the IM foils. The lower ductility and higher modulus of the DC foils appear to reflect the properties of the as-cast strip.

Table 7.9. Tensile Properties of CP-Ti Strip and Foils

Sample ID	Direction	UTS	YS	E	e_{total}	$e_{plastic}$
		MPa	MPa	GPa	%	%
IM/CR foil	longitudinal	459	339	83	32.0	31.5
IM/CR foil	transverse	438	362	87	29.1	28.7
DC strip	longitudinal	411	323	108	14.2	13.8
DC strip	transverse	401	314	107	11.1	10.7
DC/CR foil	longitudinal	413	289	96	19.3	18.9
DC/CR foil	transverse	417	325	107	18.0	17.7

Key: IM = ingot metallurgy; DC = direct cast; CR = cold rolled and annealed

Ti-1.2Al-0.8V alloy. The 50% cold rolling reduction removed the surface irregularities from Strip A. Cold rolling resulted in breakup and elongation of the primary beta and alpha grains, Figure 7.17a. Annealing in the alpha field at 700°C for 2 hours resulted in recrystallization of alpha grains and formation of beta particles (black) stabilized by impurities, Figure 7.17b. The coarse primary beta grains in the cast structure appeared to be completely broken up. An additional 50% cold reduction of strip A (75% total reduction) resulted in elongated grains of alpha, Figure 7.17c. The microstructure after final annealing at 700°C consisted of equiaxed alpha grains and beta particles, Figure 7.17d.

Strip B was 3.2-m-long with an average width of 96 mm. Strip B was cast on a peened chill roll surface. Strip B exhibited better rollability than Strip A due to the integrity across the width of the cast strip. Strip B was also fully dense with acicular alpha, serrated alpha and beta phases in the cast microstructure, Figure 7.18a. After 75% cold reduction, the alpha and beta grains were elongated in the rolling direction, Figure 7.18b. Final annealing at 700°C also produced a fine, equiaxed alpha grain structure with beta particles, Figure 7.18c.

The chill cast side of the foil rolled from strip B exhibited a bright appearance associated with a smooth surface Figure 7.19a; by contrast, the free cast side of the foil B was relatively rough and exhibited a matte appearance Figure 7.19b. The average surface roughness R_a and mean roughness depth R_z are presented in Table 7.10 for strip A and foils A & B. The average surface roughness of the as-cast strip ranged from 2.5μm to 3μm. After cold rolling, the average surface roughness of the foils was 0.17μm or less.

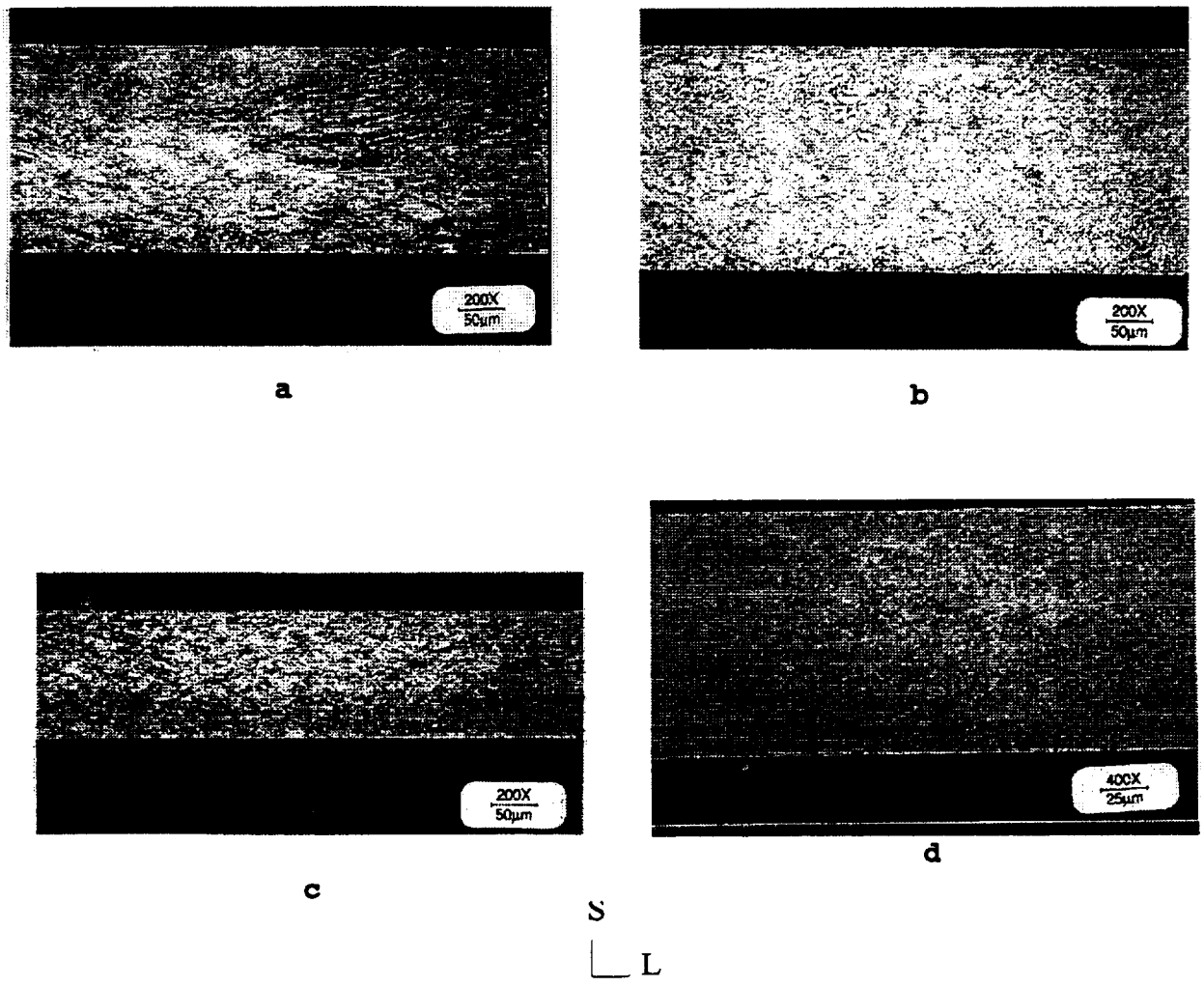

Figure 7.17: Optical micrographs of cold rolled Foil A, a) after 50% cold deformation; b) cold rolled and annealed; c) after approximately 75% cold deformation; and d) after final annealing. Rolling direction is horizontal, thickness is vertical.

The surface roughness of the cast strip was greatly reduced by cold rolling. In all cases, the transverse roughness was slightly greater than the longitudinal roughness, as a result of unidirectional rolling. The free cast surface also appeared to remain slightly rougher than the chill cast surface after cold rolling.

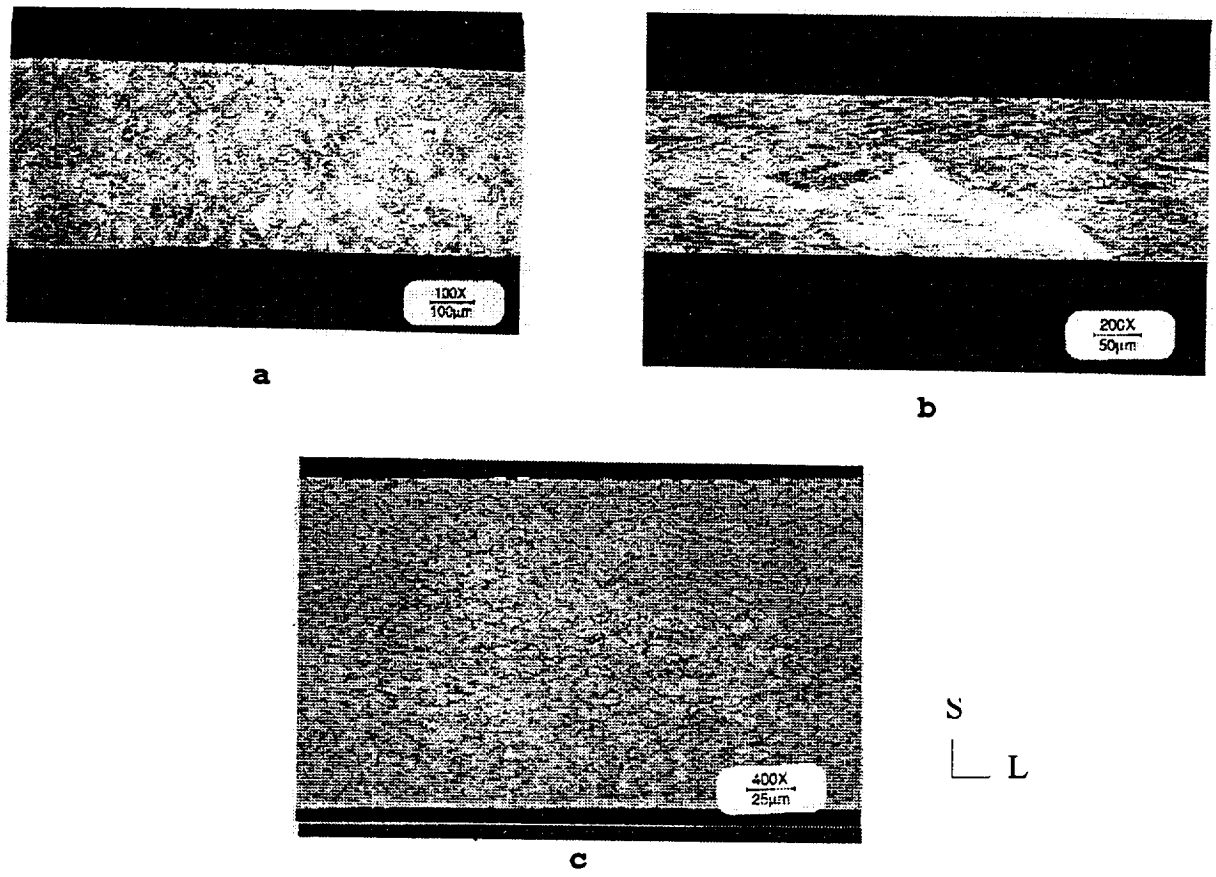

Figure 7.18. Optical micrographs of direct cast Strip B, a) as-cast; b) after approximately 75% total deformation and c) after final annealing. Rolling direction is horizontal.

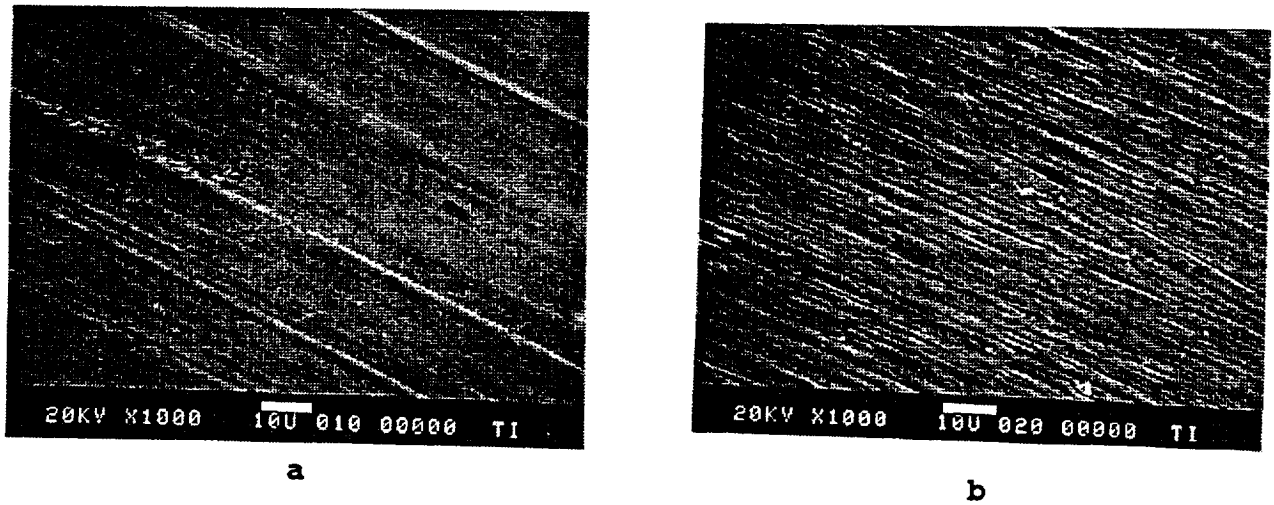

Figure 7.19. SEM micrograph illustrating surfaces of finished Foil B: (a) chill cast side; (b) free cast side.

Table 7.10. Average Surface Roughness R_a and Mean Roughness Depth R_z of Cast Strip and Cold Rolledand Annealed Foils

Sample	Side	Direction	R_a µm	R_z µm
Strip A	Roll	L	2.57	N/A
		T	2.47	N/A
Strip A	Free	L	3.02	N/A
		T	2.81	N/A
Foil A	Roll	L	0.11	0.6
		T	0.14	0.8
Foil A	Free	L	0.14	0.7
		T	0.17	0.8
Foil B	Roll	L	0.13	0.6
		T	0.14	1.0
Foil B	Free	L	0.13	0.8
		T	0.15	0.9

L = Longitudinal, T = Transverse

The carbon and gas content of Strip B as-cast and after cold rolling is presented in Table 7.11. The gas content of the strip and foil was high. Given that mixed scrap was remelted to cast the strip, the initial gas content of the scrap could not be measured. Cold rolling and vacuum annealing did not increase the interstitial content of the foils.

Table 7.11. Carbon and Gas Content of Cast Strip and Foil (wppm)

	O	N	H	C
As-cast strip	3700	510	6	300
DC/CR foil	3600	450	8	150

Key: DC = direct cast; CR = cold rolled and annealed

Wet chemical analyses were performed on the as-cast Strip B and the corresponding cold rolled Foil B. The results of the chemical analyses are presented in Table 7.12.

Table 7.12. Chemical Analysis of Cast Strip and Foil (wt %)

	Ti	Al	V	Fe
As-cast strip	97.1	1.23	0.83	0.19
DC/CR foil	96.9	1.29	0.93	0.19

Key: DC = direct cast; CR = cold rolled and annealed

Tensile tests were performed on the foils rolled from cast strips A and B. The results of the tensile tests are presented in Table 7.13. The foils exhibited high tensile strength and modulus which can be attributed, in part, to the alloy content and high interstitial content. The tensile strengths and modulus of the foils were isotropic, however, the elongation was significantly lower in the transverse direction than in the longitudinal direction due to crystalline anisotropy as a result of unidirectional rolling.

Table 7.13. Tensile Properties of Cold Rolled and Annealed Ti-1.25Al-0.8V Alloy Foils

Sample	Direction	UTS MPa	YS MPa	E GPa	e (total) %	e (plastic) %
Foil A	L	852	792	103	17.4	16.7
	T	869	838	109	7.1	6.3
Foil B	L	830	732	110	21.2	20.5
	T	804	776	115	9.1	8.4

L = Longitudinal, T = Transverse

Timetal™-1100. Three samples of cast strip were cold rolled. The cast Timetal™ - 1100 strip was cold rolled to 16% cold reduction, followed by vacuum annealing at 870°C for 2 hours. After the first rolling, sample #1 exhibited numerous cracks along the cast beta grain boundaries. The second rolling made the cracks more pronounced without increasing their number. Sample #2 exhibited single ridge line transverse cracking after the first rolling. The second rolling opened the cracks more. Sample #3 showed surface cracking (not through yet) after the second rolling. It appeared that the cracks propagated from surface microcracks found on both sides of the cast strip.

EDS analysis was performed on the cast strips (ID# 1100-5 and 1100-7) that were cold rolled and annealed. There was no significant difference in the composition of the material adjacent to cracks and voids and the material remote form the cracks and voids.

Thin film specimens, prepared by jet polishing the cold rolled and heat treated direct cast strip, were investigated in the TEM. The grain boundaries appeared to be clean as shown in Figure 7.20a. Globular precipitates with a nominal composition of 44%Ti-24%Zr-27%Si (at %) were found inside the grains but did not appear to be related to the cracking (Figure 7.20b). The silicide precipitates probably formed during vacuum heat treatment following cold rolling since no precipitates were found in the as-cast Timetal™-1100 strip.

It is not clear why there were microcracks on the chill cast surface of the Timetal™-1100 cast strip and not on the chill cast surface of the Ti-6Al-2Sn-4Zr-2Mo alloy strip which had a similar chemical composition and processing history. There was no evidence of microsegregation of silicon or other elements in the as-cast Timetal™-1100 alloy strip from the EDS analysis. The cracks in cast Timetal™-1100 were found along beta grain boundaries which suggested that cracking occurred at temperatures above the beta transus as the hot strip cooled on the chill roll or on the conveyor. As the temperature of the strip fell below the beta transus, the microstructure transformed to the alpha microstructure that was examined in the TEM.

(a)

(b)

Figure 7.20: TEM micrographs of (a) grain bounaries and (b) Ti_2ZrSi precipitate in cast, cold rolled and annealed Timetal™-1100 strip

Ti-6Al-2Sn-4Zr-2Mo alloy. Chemical analyses were performed on the DC/CR and IM/CR Ti-6242 alloy foils and the results are shown in Table 7.14. Plasma arc melting may have resulted in the evaporation of aluminum and zirconium in the DC/CR foils, but the losses did not appear to be significant.

Table 7.14. Chemical analysis of Ti-6242 alloy foils (weight %).

Element:	IM/CR FOIL	DC/CR FOIL
Titanium	85.2	85.8
Aluminum	6.05	5.89
Tin	2.02	2.02
Zirconium	4.16	3.67
Molybdenum	2.07	2.05

Key: IM = ingot metallurgy; DC = direct cast; CR = cold rolled and annealed

The carbon and gas content of the IM/CR and DC/CR foils were measured and presented in Table 7.15. The DC/CR foils exhibited higher gas content but lower carbon content than the IM/CR foils.

Table 7.15. Carbon and Gas Content of Ti-6242 Alloy Foils (wt ppm).

Element:	IM/CR FOIL	DC/CR FOIL
Carbon	570	480
Oxygen	1560	1810
Nitrogen	20	80
Hydrogen	58	90

Key: IM = ingot metallurgy; DC = direct cast; CR = cold rolled and annealed

The microstructure of the direct cast and cold rolled Ti-6-2-4-2 foil was compared to the microstructure of conventional ingot metallurgy foil in the box photomicrographs, Figure 7.21. The microstructure of the direct cast foils was more isotropic than the ingot metallurgy foil. Both materials exhibited fine, equiaxed grains, smaller than number 10, ASTM E-112.

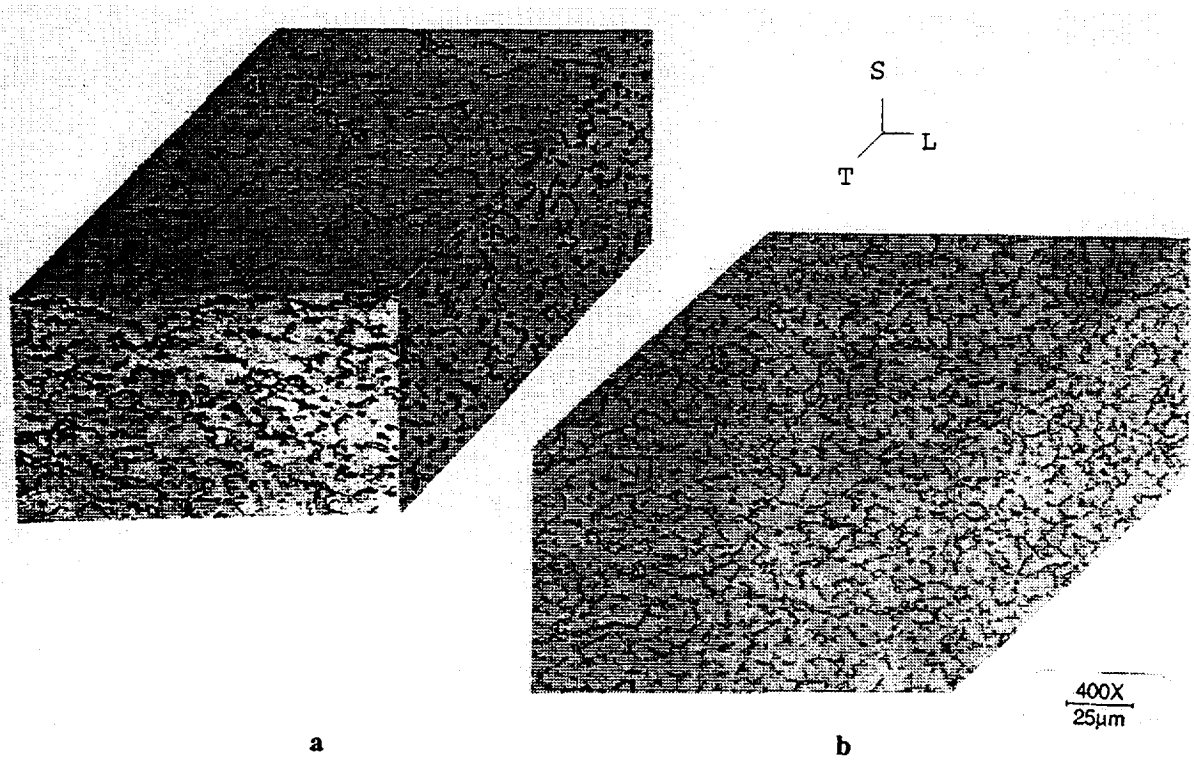

Figure 7.21: Optical microstructure of cold rolled and vacuum annealed Ti-6Al-2Sn-4Zr-2Mo foil: (a) Conventional material; (b) Direct cast material Rolling direction is horizontal in both micrographs.

The porosity on the free cast surface of the as-cast Ti-6Al-2Sn-4Zr-2Mo alloy strip was greater than on the free-cast surface of the Timetal-1100 alloy strip, yet Ti-6242 could be cold rolled to foil gauge without cracking. Crack propagation may have been more dependent on the ductility and mechanical properties of the alloy than on the surface imperfections alone. In other words, the Ti-6242 alloy may have been rollable, without cracking, because it had higher ductility and lower strength and hardness than the Timetal-1100. Surface defects were present in the cast Ti-6242 alloy, but it could be cold rolled to foil gauge because the material was more forgiving.

The tensile properties of the direct cast (DC) and ingot metallurgy (IM) foils were measured and are shown in Table 7.16. The DC foils exhibited higher strength and lower ductility than the IM foils.

Table 7.16. Tensile Properties of Cold Rolled and Annealed Ti-6242 Alloy Foils

Sample ID	UTS	YS	E	e_{total}	$e_{plastic}$
	MPa	MPa	GPa	%	%
IM Longitudinal	900	869	101	17.5	16.8
IM Transverse	893	863	108	15.4	14.7
DC Longitudinal	998	910	102	10.9	10.0
DC Transverse	1007	952	117	8.9	8.1

Key: IM = ingot metallurgy; DC = direct cast

Ti-11Al-40Nb Alloy. The material used in the cold rolling investigation was direct cast strip of Ti-11Al-40Nb intermetallic alloy (strips O-7 and O-9) and conventional Ti-11Al-40Nb 0.5-mm-thick wrought strip. Prior to rolling, the cast strips were ground from both sides from an initial thickness between 0.7-mm-thick and 0.9-mm-thick to thickness between 0.6-mm-thick and 0.8-mm-thick.

Examination of the cross-sections of the precursor strip revealed that 25 to 40 percent of the thickness of the strip had a dendritic structure, as shown in the box micrograph, Figure 7.22a. The strip solidified from the chill-cast surface to the free cast surface which resulted in the dendritic microstructure being aligned across the thickness of the strip. Along the free cast surface, a partial transformation to a coarser, dendritic grain structure appeared to have taken place. By contrast, the wrought precursor had a more equiaxed structure as shown in Figure 7.22b.

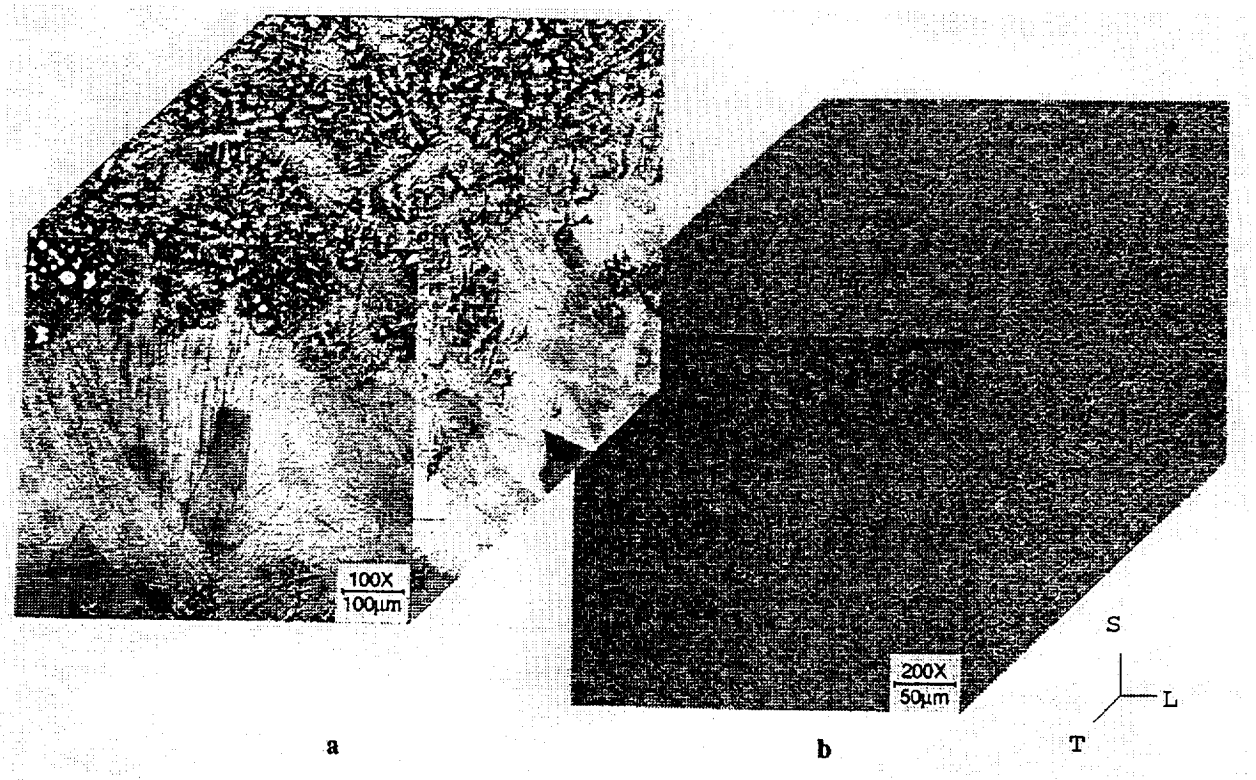

Figure 7.22: Optical block micrographs of precursor strip: (a) Cast; (b) Conventional. Longitudinal/Rolling direction is horizontal.

Results of microhardness tests along the primary rolling direction (L) and transverse direction (T) of both the wrought and cast precursor strips before and after cold rolling and thermal treatment were summarized in Table 7.17. There was not much variation in microhardness between the longitudinal and transverse test directions of each sample. By contrast, microhardness values show a much stronger variation between the wrought precursor and direct cast precursor strips. After cold rolling and annealing, the variation in microhardness between the wrought and cast foils was greatly reduced. Similar behavior was observed in other materials which have been heavily cold rolled and annealed

Table 7.17. Microhardness of Ti-11Al-40Nb Alloy Strips and Foils (VHN, 100g load)

Condition	Longitudinal	Transverse
IM Strip	336 - 376	n/a
DC Strip	391 - 413	387 - 407
IM/CR Foil	333 - 356	334 - 352
DC/CR Foil	337 - 343	322 - 327

Key: IM = ingot metallurgy; DC = direct cast; CR = cold rolled and annealed

The dendritic B2 microstructure of the cast precursor strip was transformed after cold reduction of approximately 82% followed by heat treatment (Figure 7.23a). Cold rolling and annealing refined the relatively coarse cast microstructure to a very fine, transformed, three-phase microstructure with some banding parallel to the transverse rolling direction. By contrast, the microstructure of the ingot metallurgy foil shown in Figure 7.23b, resembled the microstructure of the wrought strip precursor, (Figure 7.22b), but had coarsened after cold rolling and heat treatment.

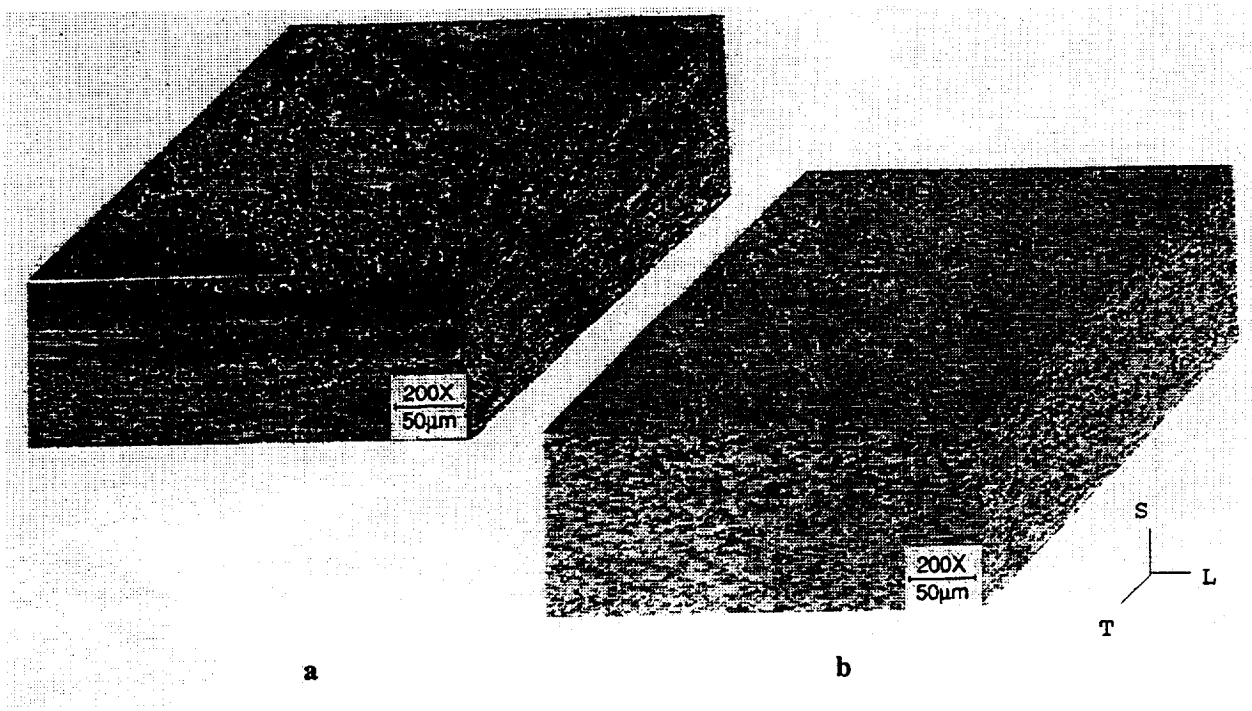

Figure 7.23: Optical micrographs illustrating microstructures developed in cold rolled and annealed Ti-11Al-40Nb material: (a) Cast; (b) Conventional. Rolling direction is horizontal in both micrographs.

TEM analysis of thin foil specimens of both the ingot metallurgy foils (Figure 7.24a) and the cast and cold rolled foils (Figure 7.24b) revealed a three phase microstructure. The microstructure consisted of equiaxed primary $\alpha 2$ grains; orthorhombic platelets; with the B2 phase along the grain boundaries. The three phases were identified by EDS analysis (Figure 7.24c-e).

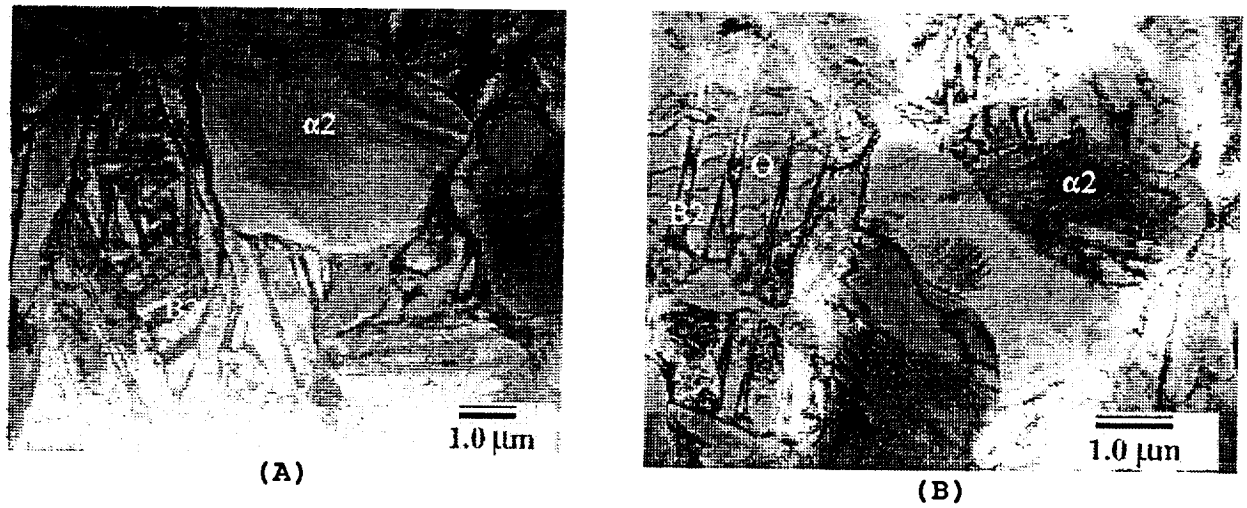

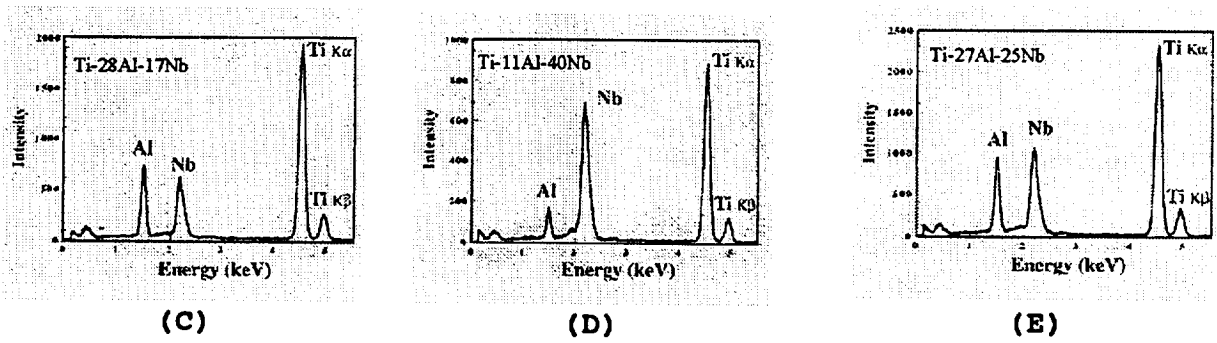

Figure 7.24: TEM micrographs of (a) conventional ingot metallurgy (b) cast, rolled and annealed Ti-11Al-40Nb alloy foils.

Some areas in the primary α2 grains had transformed into an extremely fine banded structure consisting of α2 and orthorhombic phases (Figure 7.25). Such faulting has not been seen before in α2. The displacement vector that is characteristic of the faults lies in the basal plane (0001) whereas the faults lie normal to the basal plane. Select area diffraction patterns (Figure 7.26) showed streaking due to the prescence of the faulted area. The origin of the faulted zone is not well understood, but it may be related to the transformation from the α2 phase to the orthorhombic phase.

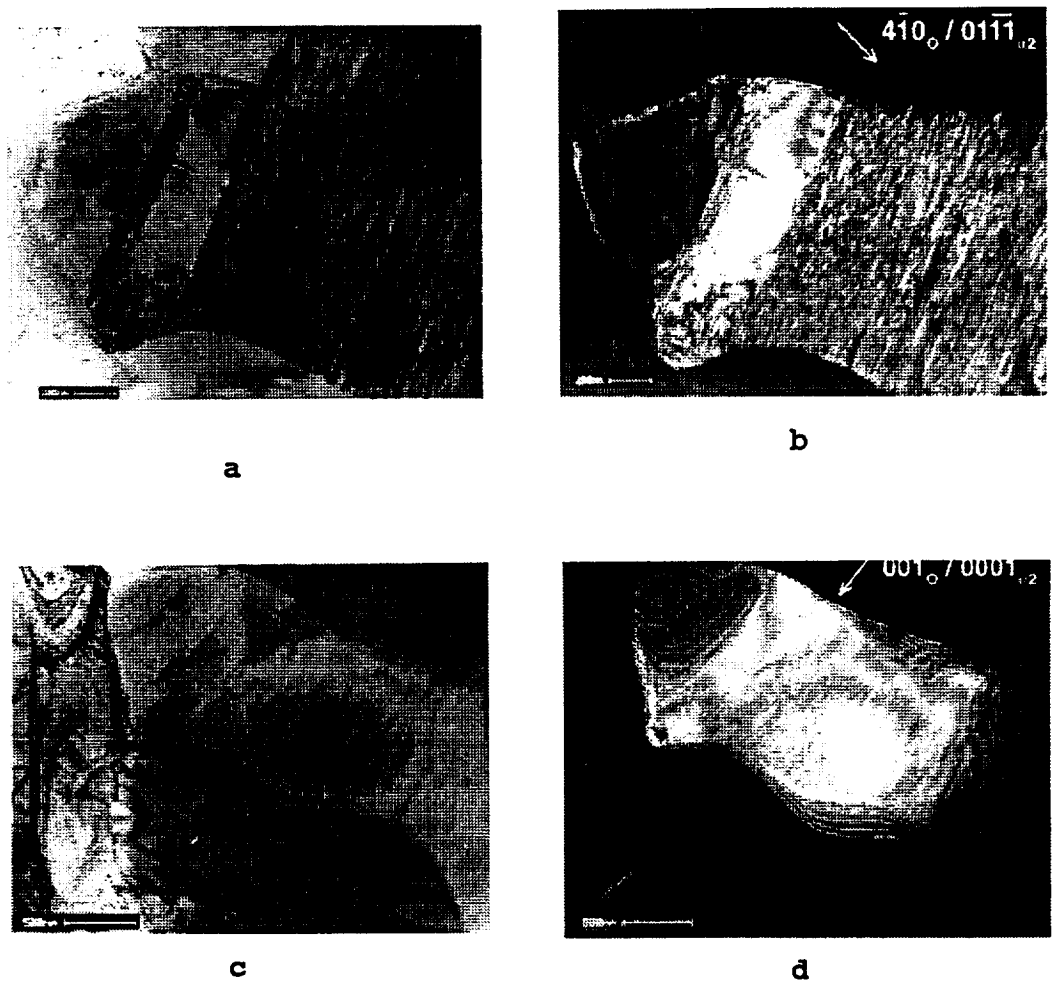

Figure 7.25: TEM micrographs showing faulted α2 (a) bright field image (b) dark field image and invisibility of faulted area (c) bright field image, (d) dark field image in direct cast, cold rolled and annealed Ti-11Al-40Nb alloy foil.

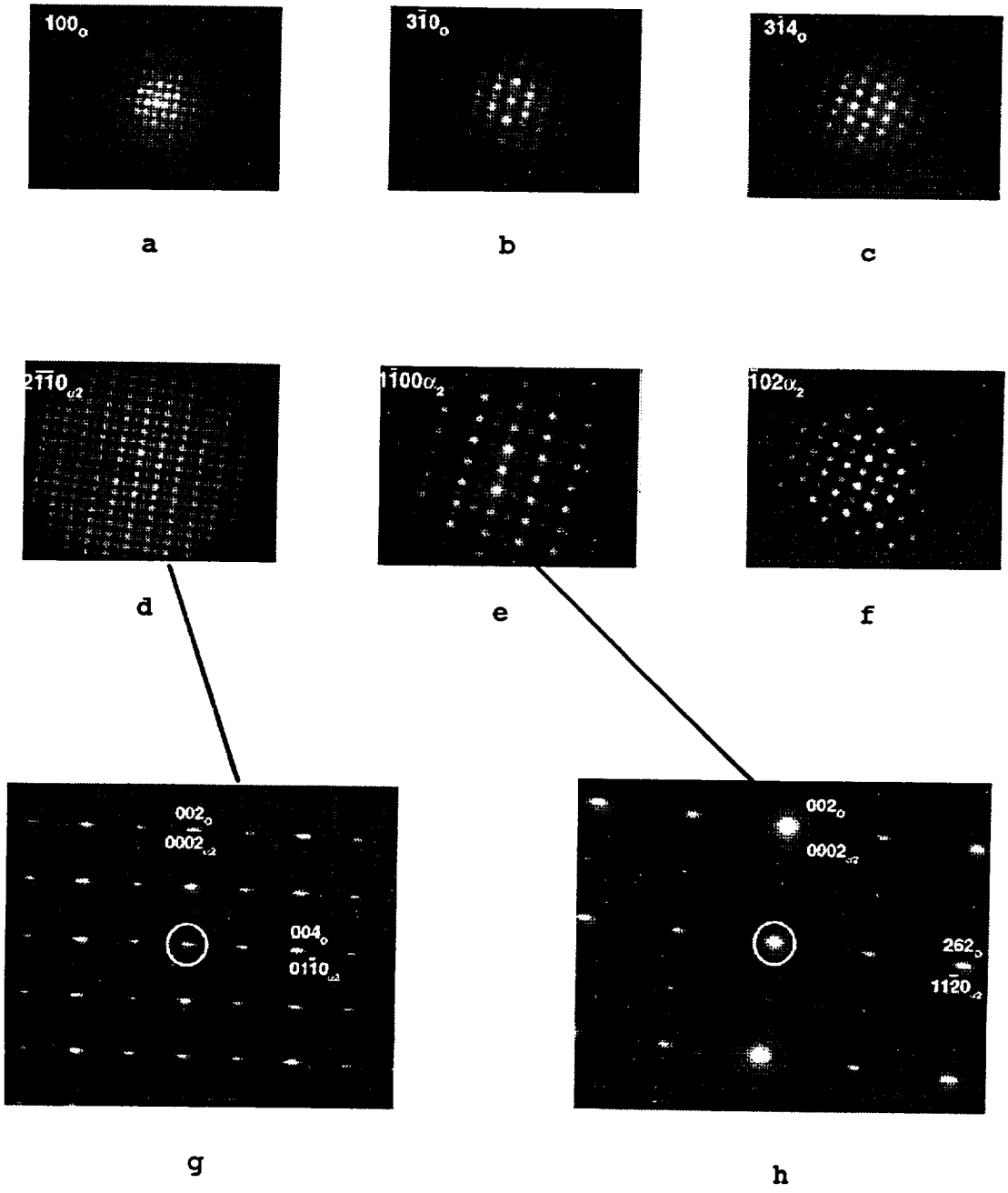

Figure 7.26: Selected area diffraction patterns of (a)-(c) Orthorhombic phase and (d)-(h) "faulted" α2 in direct cast, cold rolled and annealed Ti-11Al-40Nb alloy foil.

8.0 CONCLUSIONS

The plasma melt overflow furnace produced 0.5-mm-thick by 100-mm-wide strips up to 3-m-long. Strips were successfully cast from commercially pure titanium (CP-Ti) and five different titanium alloys: Ti-1.25Al-0.8V alloy; Timetal™-1100 alloy; Ti-6Al-2Sn-4Zr-2Mo. alloy; Ti-11Al-40Nb (orthorhombic Ti-aluminide); and Ti-30.8Al-4.7Nb-2.6Cr (γ Ti-aluminide). The standoff distance between the copper hearth and the chill roll was found to play an important role in cast strip quality: generally, the best quality strips were cast at a rate of 1 m/s on a peened molybdenum chill roll with a casting time of 3 to 4 seconds.

The strips varied in thickness both across the width and length of each casting. The free cast surfaces were typically rougher than the chill-cast surfaces. Micro-cracks were found on the chill-cast surfaces of all Timetal™-1100 alloy strips, but micro-cracks where not found on other alloys. Surface connected porosity on the free-cast side was characteristic of all alloys except CP-Ti and Ti-1.25Al-0.8V alloy. The porosity was found between primary grains and related to strip solidification.

The chemical purity of the cast strip was quite good. The strips consistently exhibited low carbon and gas contents: typically, plasma arc melting and strip casting resulted in less than 100 wppm increase in interstitial oxygen in all titanium alloys evaluated. Slight aluminum losses were measured in the cast Ti-aluminide strips when compared to the starting ingot materials.

A wire mesh belt conveyor collected the strip after casting which improved the uniformity of secondary cooling of the cast strip and substantially improved strip flatness. The cast strip required creep flattening before pack rolling but as-cast strips could be cold rolled without flattening.

Pack rolling of the γ Ti-aluminide cast strip was unsuccessful. The pack design proved to be of critical importance during hot pack-rolling of thin γ Ti-aluminide preforms. Decreasing the pack cover thickness reduced the secondary stresses induced by rolling a harder material in a softer can. Selection of a capsule material with high temperature deformation characteristics closer to γ Ti-aluminide than the Ti-6Al-4V alloy used during this investigation might further reduce the secondary stresses during hot pack-rolling.

The CaO release agent used during hot pack-rolling appeared to have reacted with the surface of both the direct cast (DC) and ingot metallurgy (IM) γ Ti-aluminide preforms to form a coarse-grained, brittle surface layer that nucleated cracks which propagated through the thickness of the preforms. The preforms cut from direct cast γ Ti-aluminide strip exhibited surface porosity and thickness variation that may have acted as crack nucleation sites in addition to the brittle reaction layer formed from contact with the CaO release agent. Grinding of the cast surfaces could be performed (as it was with wrought preforms IM-3 and IM-4) to remove the surface imperfections. There was no evidence of coarse grains or flaws at the surfaces of wrought γ preforms encapsulated with a CaF_2 release agent, however. Thus, one

might conclude that the CaF_2 parting agent did indeed have a beneficial effect on the rollability of γ Ti-aluminide preforms. Future efforts should thus be directed at optimizing the capsule materials and design, optimizing the release agent, surface grinding the DC preforms to eliminate surface imperfections and refining the pack-rolling practices.

The technical feasibility of using cold rolling in a cold rolling and annealing sequence to fabricate foils from direct cast titanium strip was successfully demonstrated. Cast strips of CP-Ti, Ti-1.25Al-0.8V alloy, Ti-6Al-2Sn-4Zr-2Mo alloy and Ti-11Al-40Nb orthorhombic Ti-aluminide were successfully cold rolled to foil gauge. Cold rolling greatly reduced the surface roughness associated with the as-cast strip. Surface connected porosity found in several cast strips was healed by cold rolling. Fully dense foils were produced.

Cold rolling and annealing resulted in recrystallization and refinement of the cast microstructures. The cast, cold rolled and annealed foils exhibited fine, equiaxed microstructures comparable to the microstructures of conventional ingot metallurgy foils. The cast, cold rolled and annealed foils exhibited high tensile strength and elastic modulus but lower elongation than comparable ingot metallurgy foils.

High quality titanium foils were produced from direct cast strip that was cold rolled and annealed. The feasibility of casting 300-mm-wide titanium strip using MORST was demonstrated in a previous project [5]. Therefore, the MORST process can be scaled-up to commercial widths. Melting capacity must be increased to allow longer and wider strips to be cast. In addition, a system like a belt wrapper to coil the strip, needs to be developed. Further improvements in reducing thickness variations in the as-cast strip will be needed before commercialization, or a light surface grinding after casting will be required before cold rolling. It is anticipated that the full economic benefits of this technique will be realized when coils of titanium strip are cast to allow coil-to-coil cold rolling.

Acknowledgments

The authors would like to thank Brian Judd at Ribtec for his assistance in operating the plasma melt overflow furnace and casting the titanium strip; Mr. Don Larsen at Howmet for creep flattening the γ pack rolling samples; Dr. Jan Ringnalda and Dr. Vincent Hou at OSU for their assistance with TEM sample preparation and electron microscopy.

References

1. T.A. Gaspar, J.M. Newman, E. Batawi and J.A. Peters, "Producing Foils from Direct Cast Titanium Strip" (Final Report NASA Contract NAS1-19541, 1992).

2. T.A. Gaspar, L.E. Hackman, E. Batawi and J.A. Peters, "Effects of Thermomechanical Processing on Titanium Aluminide Strip Cast by the Melt Overflow Process", Materials Science and Engineering, A179/A180 (1994) 645-648.

3. T.A. Gaspar, "Rotatable Crucible for Rapid Solidification Process", U.S. Patent 4,907,641, (1990).

4. I.M. Sukonnik, S.L. Semiatin, and M. Haynes, "Effect of Texture on the Cold Rolling Behavior of an Alpha-Two Titanium Aluminide", Scripta Metallurgica and Meterialia, 26 (6) (1992) 993-998.

5. T.A. Gaspar, L.E. Hackman, M. Aindow and H.L. Fraser, "Direct Cast Titanium Alloy Strip", Report number WRDC TR-90-4071, Materials Laboratory, Wright-Patterson AFB OH.

REPORT DOCUMENTATION PAGE

Form Approved
OMB No. 0704-0188

1. AGENCY USE ONLY (*Leave blank*)	2. REPORT DATE	3. REPORT TYPE AND DATES COVERED
	May 1996	Contractor Report (March 1993-March 1995)

4. TITLE AND SUBTITLE
Producing Foils From Direct Cast Titanium Alloy Strip

5. FUNDING NUMBERS
C NAS1-19942
WU 505-63-50-02

6. AUTHOR(S)
T.A.Gaspar, T.A.Stuart, I.M. Sukonnik, S.L. Semiatan, E. Batawi
J.A. Peters, H.L. Fraser

7. PERFORMING ORGANIZATION NAME(S) AND ADDRESS(ES)
Ribbon Technology Corporation
Columbus, OH 43230

8. PERFORMING ORGANIZATION REPORT NUMBER

9. SPONSORING / MONITORING AGENCY NAME(S) AND ADDRESS(ES)
NASA Langley Research Center
Hampton, VA 23681-0001

10. SPONSORING / MONITORING AGENCY REPORT NUMBER
NASA CR-4742

11. SUPPLEMENTARY NOTES
Langley Technical Monitor: William D. Brewer

12a. DISTRIBUTION / AVAILABILITY STATEMENT
Unclassified - Unlimited
Subject Category 26

12b. DISTRIBUTION CODE

13. ABSTRACT (*Maximum 200 words*)

This research was undertaken to demonstrate the feasibility of producing high-quality, thin-gage, titanium foil from direct cast titanium strip. Melt Overflow Rapid Solidification Technology (MORST) was used to cast several different titanium alloys into 500 μm thick strip, 10 cm wide and up to 3 m long. The strip was then either ground, hot pack rolled or cold rolled, as appropriate, into foil. Gamma titanium aluminide (TiAl) was cast and ground to approximately 100 μm thick foil and alpha-2 titanium aluminide (Ti3Al) was cast and hot pack rolled to approximately 70 μm thick foil. CP Ti, Ti-6-Al-2Sn-4Zr-2Mo, and Ti-22Al-23Nb (Orthorhombic), were successfully cast and cold-rolled into good quality foil (<125 μm thick). The foils were generally fully dense with smooth surfaces, had fine, uniform microstructures, and demonstrated mechanical properties equivalent to conventionally produced titanium. By eliminating many manufacturing steps, this technology has the potential to produce thin gage, titanium foil with good engineering properties at significantly reduced cost relative to conventional ingot metallurgy processing.

14. SUBJECT TERMS
titanium, foil, casting, melt-overflow

15. NUMBER OF PAGES
66

16. PRICE CODE
A04

17. SECURITY CLASSIFICATION OF REPORT	18. SECURITY CLASSIFICATION OF THIS PAGE	19. SECURITY CLASSIFICATION OF ABSTRACT	20. LIMITATION OF ABSTRACT
Unclassified	Unclassified		